



TÉCNICO
LISBOA



Life Cycle Assessment of Lithium-Sulphur Batteries

Rachel Gabriella Sadok

Thesis to obtain the Master of Science Degree in

Energy Engineering and Management

Supervisors: Prof. Maria de Fátima Grilo da Costa Montemor
Eng. Gabriela Benveniste

Examination Committee

Chairperson: Prof. Duarte de Mesquita e Sousa

Supervisor: Prof. Maria de Fátima Grilo da Costa Montemor

Member of the Committee: Prof. Maria Amélia Nortadas Duarte de Almeida Lemos

November 2017

Acknowledgments

I would like to extend my deepest thanks and gratitude to my supervisor at IREC, Gabriela Benveniste, and my supervisor at IST, Maria de Fátima Grilo da Costa Montemor, for their guidance and support in writing this dissertation.

This study would also not have been possible without the help from the members of the HELIS project especially Dr. Cristina Flox Donoso and Dr. Jordi Jacas Biendicho in providing their data and knowledge on the batteries investigated.

I cannot go without thanking InnoEnergy and the SELECT Master's for supporting my studies financially, educationally, and in many ways, emotionally. The SELECT students and faculty will be a part of my family forever and I greatly appreciate all of the opportunities this experience has brought me.

Finally, to my family and boyfriend: thank you for allowing me to take this journey and thank you for enduring all the emotions I went through along this adventure. I love you and couldn't have gotten to where I am without your love and support!

Resumo

As baterias de lítio-enxofre (Li-S) emergiram como uma tecnologia promissora, com capacidade e densidade de energia teóricas maiores do que as baterias de íões de lítio usadas atualmente. No entanto, uma vez que atingir a capacidade e a densidade de energia teóricas provou ser bastante difícil, ainda não foi possível chegar à fase de comercialização. Neste projecto é feita uma análise de Avaliação do Ciclo de Vida (“Life Cycle Assessment”, LCA) em duas células de bateria Li-S, desenvolvidas com o objetivo final de serem aplicadas em veículos elétricos (EVs). Uma das células da bateria Li-S vem da investigação do projeto HELIS financiado pela União Europeia, um consórcio de 14 parceiros em toda a Europa e Israel, com o objetivo de colocar uma bateria Li-S competitiva no mercado. A outra bateria de Li-S foi desenvolvida pelo laboratório de investigação do IREC, o Instituto de Investigação em Energia da Catalunha. Em primeiro lugar, o estudo realizado pretende fazer uma análise do ciclo de vida da produção das células que permita avaliar quais dos seus componentes têm um maior impacto ambiental. A segunda parte do projecto é realizar uma análise de ciclo de vida para as baterias considerando o seu uso em veículos eléctricos, numa abordagem “cradle to grave”, onde todas as fases desde a extração de matérias primas até fim de vida das baterias são consideradas. Para isto, a unidade funcional da bateria foi definida como 22 kWh, executando 1000 ciclos e que permite que o veículo percorra uma distância de 150.000 km. Os resultados mostraram que o lítio, o aço inoxidável e o alumínio são os materiais com mais impacto na produção de células e que os materiais do banco de bateria também são altamente intensivos. Assim, o BMS deve ser investigado para envolver materiais menos intensivos. Enquanto a bateria HELIS tinha uma pegada de carbono 12% menor do que a bateria IREC, a bateria IREC teve impactos menores em muitas categorias, como toxicidade humana (66% inferior), ecotoxicidade (60-82% inferior) e depleção de ozono (64% inferior). Se o consumo de energia para produzir o cátodo na bateria IREC fosse diminuído para níveis industriais, então a bateria IREC seria a bateria mais sustentável para uso em EVs. Este estudo forneceu uma LCA adicional em baterias Li-S e uma boa base para futuros estudos de avaliação de ciclo de vida quando a tecnologia tenha amadurecido.

Palavras-chave: bateria de lítio-enxofre, avaliação do ciclo de vida, veículos elétricos, projeto HELIS, sustentabilidade

Abstract

Lithium-sulphur (Li-S) batteries have emerged as a promising battery technology, with a higher theoretical capacity and energy density than Lithium-ion (Li-ion) batteries used today. However, Li-S batteries have yet to be commercialised, as achieving the theoretical capacity and energy density has proven quite difficult. This study performs life cycle assessment (LCA) analyses on two Li-S battery cells being researched for the final aim of being applied in electric vehicles (EVs). One of the Li-S battery cells comes from the investigation of the EU-funded HELIS project, a consortium of 14 partners across Europe and Israel, with the aim of bringing a competitive Li-S battery to market. The other Li-S battery cell comes from IREC's (Catalonia Institute for Energy Research) own research lab. The first objective of the study is to perform a cradle to gate LCA on just the cell production to evaluate which parts of the cells have the highest environmental impact. The second objective of the study is to perform a cradle to grave LCA on two battery systems for use in EVs where all phases from the extraction of raw materials to the end of life of the battery are considered. This required the scaling up of the cells to battery systems, where the functional unit was decided as a 22 kWh battery that would run 1000 cycles and allow the EV to go a distance of 150.000 km. The results showed that lithium, stainless steel, and aluminium were the highest impact materials in the cell production and that the battery pack materials are highly intensive as well. Thus, the BMS should be investigated to involve less-intensive materials. While the HELIS battery had a 12% lower carbon footprint than the IREC battery, the IREC battery had lower impacts in many categories such as human toxicity (66% lower), ecotoxicity (60-82% lower), and ozone depletion (64% lower). If the energy consumption to produce the cathode in the IREC battery were decreased to industrial levels, then the IREC battery would be the more sustainable battery to use in EVs. This study provided an additional LCA on Li-S batteries and a good basis for future LCA studies when these batteries have matured.

Keywords: lithium-sulphur battery, life cycle assessment, electric vehicles, HELIS project, sustainability

Contents

Acknowledgments	iii
Resumo	v
Abstract	vii
List of Tables	xi
List of Figures	xiii
Nomenclature	xv
Glossary	xvii
1 Introduction	1
1.1 Motivation	1
1.1.1 HELIS Project	2
1.2 Objectives	2
1.3 Thesis Outline	2
1.4 Life Cycle Assessment	3
1.4.1 Goal and Scope Definition	4
1.4.2 Inventory Analysis	5
1.4.3 Impact Assessment	5
1.4.4 Interpretation	6
1.5 GaBi Professional Software	6
1.6 Lithium-Sulphur Batteries	7
1.6.1 Overview	7
1.6.2 Comparison with Li-ion Batteries	8
1.7 Literature Research	9
2 Implementation	11
2.1 Goal and Scope	11
2.1.1 Purpose	11
2.1.2 Definition of the System	12
2.1.3 System Boundaries	12
2.1.4 Functional Unit	12
2.1.5 Selection of the Impact Categories	12

2.1.6	Limitations	13
2.1.7	Main Assumptions	13
2.2	Life Cycle Inventory	15
2.2.1	HELIS Cells	15
2.2.2	IREC Coin Cells	16
2.3	Parameters	17
2.4	Equivalency for Comparison	17
2.4.1	Battery Pack	18
2.4.2	Equivalency Parameters	18
2.5	Use Phase	19
3	Results	21
3.1	Life Cycle Impact Assessment and Interpretation for Cradle to Gate Analysis	21
3.1.1	HELIS Cell	21
3.1.2	IREC Cell	24
3.2	Life Cycle Impact Assessment and Interpretation for Cradle to Grave Analysis	28
3.2.1	HELIS Battery	28
3.2.2	IREC Battery	31
3.2.3	Battery Comparison	31
3.3	Sensitivity Analyses	33
3.3.1	Energy Density	34
3.3.2	Cathode Production Energy Consumption	35
3.3.3	Cathode Binders	36
4	Conclusions	39
4.1	Achievements	39
4.1.1	Summary of Results	40
4.1.2	Lessons Learned	41
4.2	Future Work	41
	Bibliography	43
A	GaBi Process Flows: HELIS Battery	47
B	GaBi Process Flows: IREC Battery	51

List of Tables

1.1	Comparison between Li-S and Li-ion Batteries.	8
2.1	The eleven different impacts assessed in this LCA.	13
2.2	Material inventory for the HELIS battery cell.	16
2.3	Material inventory for the IREC battery cell.	16
2.4	Parameters of the two battery cells.	17
2.5	Material inventory for the IREC cylindrical cell.	17
2.6	Parameters used in the calculation of the number of cells in a battery.	18
2.7	Material inventory for the battery pack for the two battery systems.	18
2.8	Parameters of the equivalency of the two batteries.	19
3.1	LCIA results for the HELIS battery cell (cradle to gate analysis) categorised by stream. . .	22
3.2	LCIA results for the HELIS battery cell (cradle to gate analysis) categorised by cell part. .	22
3.3	LCIA results for the IREC battery cell (cradle to gate analysis) categorised by stream. . .	25
3.4	LCIA results for the IREC battery cell (cradle to gate analysis) categorised by cell part. . .	26
3.5	LCIA results for the HELIS battery (cradle to grave analysis) categorised by phase of life. .	29
3.6	LCIA results for the IREC battery (cradle to grave analysis) categorised by phase of life. .	31
3.7	LCIA results for the HELIS and IREC battery systems (cradle to grave analysis).	32
3.8	Results for the sensitivity analysis on energy density of the IREC cylindrical battery. . . .	34
3.9	Results for the sensitivity analysis on cathode production energy consumption.	35
3.10	Results for the sensitivity analysis on cathode binder in the HELIS cells.	37

List of Figures

1.1	The framework of the LCA is shown, comprising of the four main steps [7].	3
1.2	This LCI table shows the process of setting up the Life Cycle Inventory [7].	5
1.3	A scheme of the Li-S cell displaying the lithium metal anode, sulphur-based cathode, separator, and electrolyte [15].	8
2.1	Schematic displaying the methodology of open-loop recycling [24].	14
2.2	Photos of the first prototype HELIS cells.	16
2.3	Photos of the cells manufactured by IREC (left) and their parts (right).	16
2.4	The EU-28 electricity mix as of 2015 (% of total, based on GWh) [32].	20
3.1	Pie chart displaying the contributions of each part of the HELIS cell production to global warming potential in percentages.	23
3.2	Pie chart displaying the contributions of each part of the HELIS cell production to primary energy demand in percentages.	24
3.3	Pie chart displaying the contributions of each part of the HELIS cell production to human toxicity potential in percentages.	25
3.4	Pie chart displaying the contributions of each part of the IREC cell production to global warming potential in percentages.	26
3.5	Pie chart displaying the contributions of each part of the IREC cell production to primary energy demand in percentages.	27
3.6	Pie chart displaying the contributions of each part of the IREC cell production to ozone depletion potential in percentages.	28
3.7	Pie chart displaying the contributions of each phase of the life cycle of the HELIS battery to global warming potential in percentages.	29
3.8	Pie chart displaying the contributions of each phase of the life cycle of the HELIS battery to marine aquatic ecotoxicity potential in percentages.	30
3.9	Pie chart displaying the contributions of each phase of the life cycle of the HELIS battery to terrestrial ecotoxicity potential in percentages.	30
3.10	Graph showing the comparison between the HELIS and IREC batteries for global warming potential.	32

3.11 Graph showing the comparison between the HELIS and IREC batteries for human toxicity potential.	33
3.12 Graph showing the comparison between the HELIS and IREC batteries for primary energy demand.	33
3.13 Graph showing the comparison between the four IREC batteries with varying energy densities and the HELIS battery for global warming potential.	34
3.14 Graph showing the comparison between the two batteries when the energy consumption of the cathode of the IREC battery is equated to that of the HELIS battery for freshwater aquatic ecotoxicity.	36
3.15 Graph showing the comparison between the two cathode binders in the HELIS battery cell for global warming potential.	37
A.1 The GaBi process flow is displayed for the cradle to grave model of the HELIS battery. . .	47
A.2 The GaBi process flow is displayed for the cathode of the HELIS battery.	48
A.3 The GaBi process flow is displayed for the electrolyte of the HELIS battery.	48
A.4 The GaBi process flows are displayed for the anode of the HELIS battery [left] and the separator of the HELIS battery [right].	49
A.5 The GaBi process flow is displayed for the cell casing of the HELIS battery.	49
A.6 The GaBi process flow is displayed for the battery pack (the same materials were used for the two battery systems).	49
B.1 The GaBi process flow is displayed for the cradle to grave model of the IREC battery. . . .	51
B.2 The GaBi process flow is displayed for the cathode of the IREC battery.	52
B.3 The GaBi process flow is displayed for the carbon nanofibers produced for the cathode of the IREC battery.	52
B.4 The GaBi process flows are displayed for the anode of the IREC battery [left] and the separator of the IREC battery [right].	52
B.5 The GaBi process flow is displayed for the electrolyte of the IREC battery. It only consists of transport since it is the same electrolyte used as in the HELIS battery.	53
B.6 The GaBi process flow is displayed for the gasket of the IREC battery.	53
B.7 The GaBi process flow is displayed for the spacer of the IREC battery.	53
B.8 The GaBi process flow is displayed for the spring of the IREC battery.	54
B.9 The GaBi process flow is displayed for the cell casing of the IREC battery.	54
B.10 The GaBi process flow is displayed for the battery pack of the IREC battery.	54

Nomenclature

ADP Abiotic Depletion Potential.

AP Acidification Potential.

BMS Battery Management System.

CFC Chlorofluorocarbon.

CMC Carboxymethyl Cellulose.

DME Dimethyl Ether.

ELCD European Life Cycle Database.

EOL End of Life.

EP Eutrophication Potential.

EPD Environmental Product Declaration.

EV Electric Vehicle.

FAETP Freshwater Aquatic Ecotoxicity Potential.

GHG Greenhouse Gas.

GWP Global Warming Potential.

HELIS High Energy Lithium Sulphur Cells and Batteries.

HTP Human Toxicity Potential.

IPCC Intergovernmental Panel on Climate Change.

IREC Institut de Recerca en Energia de Catalunya (Catalonia Institute for Energy Research).

ISO International Organisation for Standardisation.

LCA Life Cycle Assessment.

LCC Life Cycle Costing.

LCI Life Cycle Inventory.

LCR Life Cycle Reporting.

LCWE Life Cycle Working Environment.

Li – ion Lithium-ion.

Li – S Lithium-Sulphur.

LiTFSI Lithium bis(trifluoromethanesulphonyl)imide.

MAETP Marine Aquatic Ecotoxicity Potential.

MDP Metal Depletion Potential.

MEP Marine Eutrophication Potential.

MWCNT Multiwalled Carbon Nanotubes.

Na – ion Sodium-ion.

NCM Nickel-Cobalt-Manganese.

NMP N-methyl-2-pyrrolidone.

ODP Ozone Layer Depletion Potential.

PAH Polycyclic Aromatic Hydrocarbons.

PCB Printed Circuit Board.

PED Primary Energy Demand.

PET Polyethylene Terephthalate.

POCP Photochemical Ozone Creation Potential.

PP Polypropylene.

PVDF Polyvinylidene Fluoride.

PVF Polyvinyl Fluoride.

SBR Styrene-Butadiene-Rubber.

TEGDME Tetraethylene Glycol Dimethyl Ether.

TETP Terrestrial Ecotoxicity Potential.

TRL Technology Readiness Level.

Glossary

ADP	Abiotic Depletion Potential is an impact category that describes the reduction of the global amount of non-renewable (meaning a time-frame of 500 years) raw materials. Here the fossil ADP has been chosen which includes the fossil energy carriers (crude oil, natural gas, coal resources) listed in MJ of lower calorific value.
AP	Acidification Potential is an impact category which accounts for the acidification of soils and waters that occurs through the transformation of air pollutants into acids and leads to a decrease in the pH-value of rainwater and fog from 5.6 to 4 and below. The acidification potential is given in sulphur dioxide equivalents (SO ₂ -eq.).
CML	The CML method is a method used for the impact assessment in the LCA which was developed by Leiden University's Institute of Environmental Sciences. It uses the indices published by the Intergovernmental Panel on Climate Change (IPCC).
EP	Eutrophication Potential is an impact category which accounts for the enrichment of nutrients in a certain place. It can be aquatic or terrestrial and air pollutants, wastewater, and fertilisation in agriculture all contribute to eutrophication. The eutrophication potential is given in phosphate equivalents (PO ₄ -eq.).

Ecotoxicity	Ecotoxicity is represented in three different impact categories in this study: freshwater aquatic, marine aquatic, and terrestrial. These account for the toxicity potentials on freshwater, coastal marine water, and air and soils, respectively. These potentials were researched and collected in USEtox, a scientific consensus model under the UNEP/SETAC Life Cycle Initiative.
Functional Unit	The functional unit is the quantified definition of the function of the product in a LCA. The functional unit is critical for comparisons of two systems or products to assure that the comparison is valid.
GWP	Global Warming Potential is an impact category which accounts for the greenhouse effect that results in a warming of the earth's surface. In addition to the natural mechanism, human activities enhance the greenhouse effect. GHGs, believed to be anthropogenically caused or increased, include carbon dioxide, methane, and CFCs. Here it is measured including biogenic carbon which means that carbon dioxide taken up by plants and this carbon later released as biogenic CO ₂ or methane is accounted for. The global warming potential is given in carbon dioxide equivalents (CO ₂ -eq.).
HTP	Human Toxicity Potential is an impact category which accounts for the potential risks of adverse effects in humans via three steps: environmental fate, exposure, and effects. It is based on cancerous and non-cancerous effects derived from laboratory studies. The human toxicity potential is given in 1,4-Dichlorobenzene (C ₆ H ₄ Cl ₂) equivalents (kg DCB-eq.).

LCA	Life Cycle Assessment is an analysis of the environmental impact of a product, process, or activity over the course of its lifetime by identifying and quantifying the energy and materials used and wastes released to the environment.
ODP	Ozone Depletion Potential is an impact category which accounts for the depletion of ozone in the stratosphere caused by anthropogenic emissions. The substances which have a depleting effect on the ozone can essentially be divided into two groups: the chlorofluorocarbons (CFCs) and nitrogen oxides (NO _x). The ozone depletion potential is given in CFC 11-equivalents.
PED	Primary Energy Demand is an impact category which accounts for the quantity of energy directly withdrawn from the hydrosphere, atmosphere, or geosphere or energy source without any anthropogenic changes. Here it accounts for all energy sources, both renewable and non-renewable, and the net calorific value is used which is the higher heating value minus the heat of vapourisation of the water. The primary energy demand is given in MJ.
POCP	Photochemical Ozone Creation Potential is an impact category which accounts for the creation of ozone at ground level, also known as summer smog, which is classified as a damaging trace gas and is suspected to damage vegetation and material. High concentrations of ozone are also toxic to humans. The photochemical ozone creation potential is given in ethylene equivalents (C ₂ H ₄ -eq.).

Chapter 1

Introduction

Life cycle assessment (LCA) was performed on two different types of Lithium-Sulphur (Li-S) battery cells: ones manufactured for the EU-funded HELIS (High Energy Lithium Sulphur Cells and Batteries) project and cells manufactured in the IREC (Catalonia Institute for Energy Research) laboratories. The cell dimensions and characteristics are different, thus they were resized and combined adequately to be compared with the intention of being used in electric vehicle (EV) applications. After the analysis of the results, a decision was made on which battery, based on its chemistry and performance, is more environmentally sustainable for the application in EVs.

1.1 Motivation

This study was performed for the purposes of the HELIS project which receives funding from the European Union's Horizon 2020 research and innovation program under Grant Agreement No 666221. The HELIS project aims to develop three different series of Li-S cell prototypes to be tested for use in EVs [1]. By comparing the chemistry of the first Li-S cell prototype with Li-S cells already tested and proven in the IREC laboratories, the environmental impacts can be analysed.

LCA research on Li-S batteries is lacking since these batteries have yet to be commercialised. The first article published performing a LCA on these batteries was in March of 2017 so there is not enough research yet on the sustainability of these batteries [2]. By performing this study on two different types of Li-S battery cells currently being researched, the goal is that more awareness is brought to these types of batteries and that they are shown to be more sustainable than batteries used today.

While not much LCA research currently exists on Li-S batteries, the field of electromobility has received much attention and research globally to discover innovative ways of reducing the environmental impact of conventional vehicles. Along with EVs comes energy storage and the motivation to find clean and proper electricity storage systems. While EV sales increase every year, there still remain two key issues with the widespread use of EVs. The first issue is the limited range due to low energy density of the battery. The second issue is the high cost of batteries; the most expensive part of the EV is the battery, thus making the batteries cheaper is intrinsic to making the cost of the vehicle cheaper [3]. LCA

and other life cycle tools such as life cycle costing (LCC) help improve upon these batteries by identifying which materials and processes have higher impacts environmentally and economically.

Much of literature in the electromobility field when it comes to energy storage is dedicated to the second life of these EV batteries. Once they have lost 20% of their capacity, EV batteries are no longer considered useful for traction purposes. But these batteries still have 80% of their capacity and thus can be used for other stationary purposes [4]. LCA can be a very useful tool for identifying these possible applications since it assesses the end of life (EOL) of the battery.

Various motivations lie behind this study on Li-S batteries and hopefully this research can shed more light on the situation and propel these types of batteries to the forefront of energy storage research as a viable option in the electromobility field and elsewhere.

1.1.1 HELIS Project

The HELIS project is made up of 14 partners across Europe and Israel, all working together towards the aim of developing and bringing Li-S battery technology to technology readiness levels (TRLs) equal to or above 4. It is a continuation of the EuroLiS project, also an EU-funded collaborative project working on the potential commercialisation of Li-S battery cells. The National Institute of Chemistry in Ljubljana, Slovenia coordinates both projects [1]. As a partner of the HELIS project, IREC aids in the development of the cathode and the LCA of the cell prototypes manufactured. The first prototype of the HELIS project has been developed and they are currently working on a second prototype with improved cathode and binders.

1.2 Objectives

This study has two main objectives. The first is to analyse the environmental impacts due to the production of the coin cells from IREC and the cells from the HELIS project. As a second objective, after an adequate scaling to make both devices equivalent, the cells themselves can be compared; the different ways of manufacturing Li-S battery cells are compared to find the optimal type, chemistry, and materials of the cells that maintain high performance and are as environmentally sustainable as possible.

1.3 Thesis Outline

Section 1.4, an extensive introduction to LCA, will follow to give the reader a good basis on all factors involved in this LCA study. Then, a quick introduction to the software used is given in Section 1.5 and to Li-S batteries in Section 1.6 and this chapter will end with a brief literature research in Section 1.7.

The methodology of the study will then be presented in Chapter 2 including the goal and scope of the LCA (Section 2.1) as well as the materials inventory of the two batteries investigated (Section 2.2). The process of the equivalency of the two battery systems is then described in Section 2.4.

Next the results will be presented in Chapter 3 with the impact assessment results and interpretation in Sections 3.1 and 3.2, and results from the sensitivity analyses performed in Section 3.3.

Finally the conclusions, including the achievements of the study and future work, are presented in Chapter 4.

1.4 Life Cycle Assessment

Life Cycle Assessment (LCA) is an analysis of the environmental impact of a product, process, or activity over the course of its lifetime by identifying and quantifying the energy and materials used and wastes released to the environment [5]. There are two standards for LCA created by the International Organisation for Standardisation (ISO): ISO 14040 (Environmental management - Life cycle assessment - Principles and framework) and ISO 14044 (Environmental management - Life cycle assessment - Requirements and guidelines) [6]. LCAs have four distinct steps, shown in Figure 1.1 below.

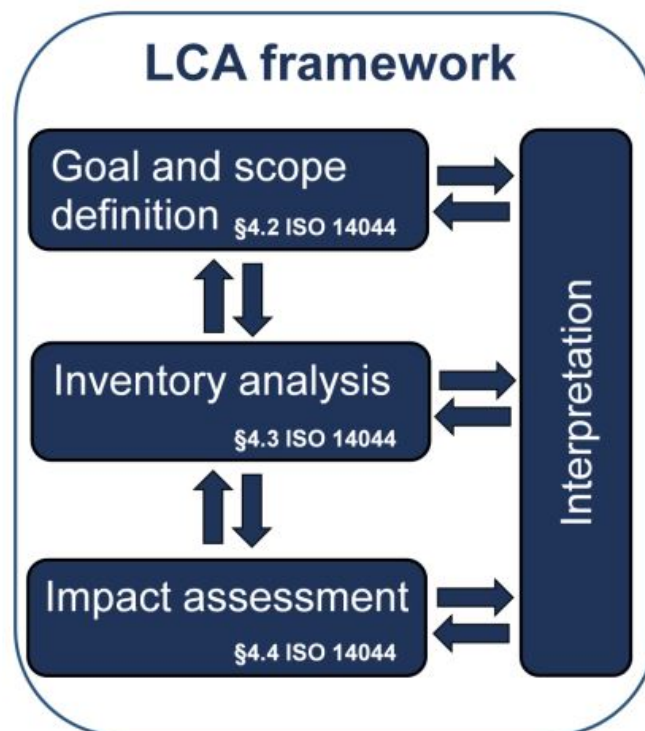


Figure 1.1: The framework of the LCA is shown, comprising of the four main steps [7].

LCA is a good tool to use in the development of a product or process to ensure the environmental impact is kept low. It points out exactly which parts or steps cause the most impact so that these can be examined and replaced or reduced if possible. LCA is based on the performance as well so that even if a product uses sustainable materials but the performance is very low, the LCA reflects that and shows the impact accordingly.

When it comes to batteries, the performance is a very important factor as well as the materials and processes used. LCA studies on the battery technology as it evolves help ensure that sustainability is accounted for every step of the way. If the performance of a battery is low, the LCA will show that through

a high environmental footprint and thus better materials can be used to increase the performance (even if they have a higher environmental impact) and the LCA can show the advantages and disadvantages of that change.

In the HELIS project, many partners work on developing higher-performing parts for the Li-S battery. By executing this LCA on the current stage of the Li-S battery, it can be seen whether these parts improve the environmental impact of the battery to make sure the development is on the right path. When the second prototype of the Li-S battery has been developed, a second LCA study can be performed to compare the two and ensure that the environmental footprint has decreased.

In the next sections of this chapter, the four main steps of the LCA - goal and scope definition, inventory analysis, impact assessment, and interpretation - will be gone through in more detail.

1.4.1 Goal and Scope Definition

In the definition of the goal the intended application, purpose, and intended audience should be clearly laid out as well as if the LCA results are meant to be used for comparative reasons. The scope definition involves characterisation of the system, definitions of all assumptions made, and explanation of the methodology used to set up the system. The scope is also where the functional unit is defined, the system boundaries are set, any data requirements are explained, limitations are stated, and many more definitions are laid out [7][8].

Functional Unit

In any LCA, a functional unit is needed especially when it comes to comparison studies. The functional unit is the quantified definition of the function of the product. When comparing two systems or products, their functional unit must be the same for the comparison to be valid [7][8].

System Boundaries

The system boundaries of the LCA define which processes are included in the system, such as the production, use, and end of life processes. There are four options when defining the system boundaries: cradle to grave, cradle to gate, gate to grave, and gate to gate. Cradle to grave is the most encompassing of the options, including the raw material extraction through the production, transportation, use, and EOL of the product. Cradle to gate includes the raw material extraction process and production process only. This is used to determine the environmental impact of the production of the product. Gate to grave entails only the use and EOL processes and is used to determine the environmental impact of the product once it is out of the factory. Finally, gate to gate is purely the production process (not including raw material extraction) and might be used to analyse a single production process's impacts [7].

1.4.2 Inventory Analysis

In this step of the LCA, the inputs and outputs for the system throughout its entire life cycle are compiled and quantified. It involves data collection and compiling the data in a Life Cycle Inventory (LCI) table, as shown in Figure 1.2 below.

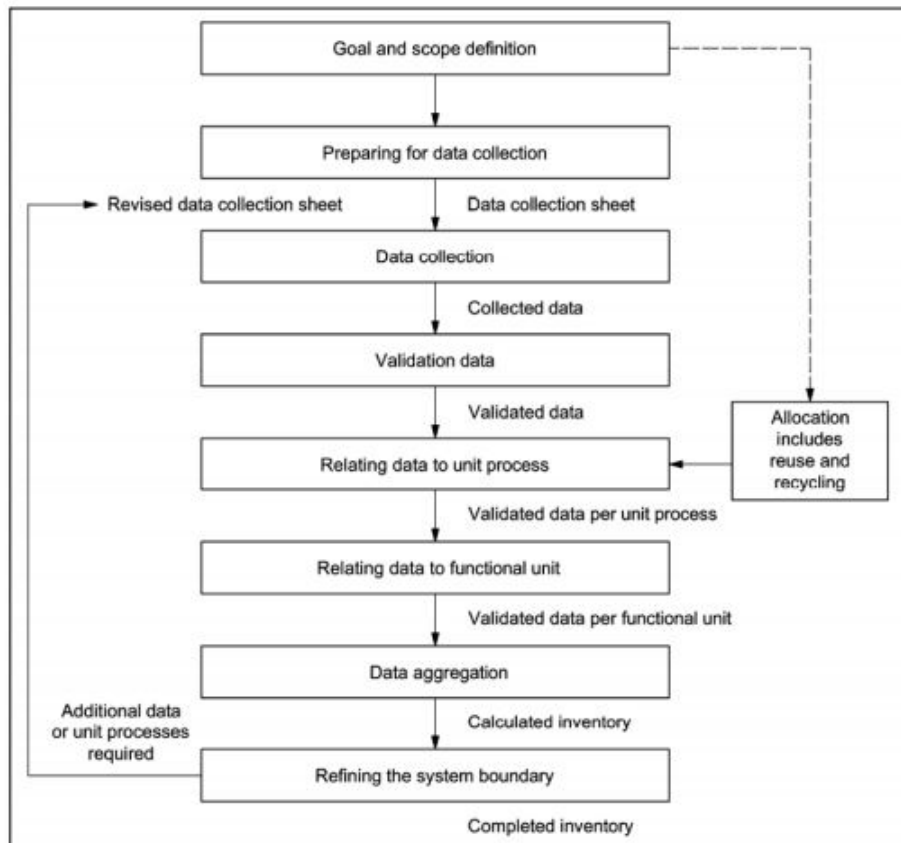


Figure 1.2: This LCI table shows the process of setting up the Life Cycle Inventory [7].

Before the LCI can be produced, three steps should be completed:

1. Data Validation: mass or energy balances can be used to validate the collected data as well as comparing to similar data.
2. Relating Data to Unit Processes.
3. Relating Data to Functional Unit.

The life cycle inventory of the overall product system is the sum of all life cycle inventories of all of the involved processes [7][8].

1.4.3 Impact Assessment

The Life Cycle Impact Assessment (LCIA) identifies and evaluates the amount and significance of potential environmental impacts arising from the life cycle inventory [7]. The various environmental impacts

include global warming potential (GWP), acidification potential (AP), eutrophication potential (EP), ozone layer depletion potential (ODP), human toxicity potential (HTP), resource depletion, ecotoxicity, and primary energy demand (PED) [8][9].

1.4.4 Interpretation

After the LCIA is performed, the results are evaluated to assure that they are consistent with the goal and scope definition and to ensure that the study has been completed. This interpretation phase encompasses two parts: identification of significant issues and evaluation [7][8].

Identification of Significant Issues

Since an extensive amount of data has been collected, it is not feasible to assess all of the data elements, so only those that contribute significantly to the outcome of the results are selected. Some types of significant issues are:

- Inventory elements (e.g. energy consumption, major material flows, wastes, and emissions).
- Impact category indicators of special interest or concern.
- Essential contributions of life cycle stages to the LCI or LCIA results (e.g. individual unit processes or groups of processes such as transportation or energy production).

The results are then presented in any convenient form (e.g. data list, table, bar diagram) and organised according to life cycle phase, different process (energy supply, transportation, raw material extraction, etc.), type of environmental impact, or other criteria [7][8].

Evaluation

To increase the reliability of the study, an evaluation consisting of three different methods is performed. First, a completeness check is done to ensure no information is missing or incomplete to satisfy the goal and scope of the study. Then, a sensitivity check is performed by evaluating how the results are affected by uncertainties in the data, calculation procedures, assumptions, etc. This check is crucial when the study involves the comparison of different alternatives to assure that significant differences or lack thereof are reliable. Finally, the consistency is checked, particularly of the used methods and the goal and scope of the study. The issues checked here include the data quality, system boundaries, impact assessment, and others [7][8].

1.5 GaBi Professional Software

GaBi Professional software is used to perform the LCA of the Li-S batteries. The GaBi software is a LCA modelling software created by the German company thinkstep, originally PE International. The name

GaBi comes from the German Ganzheitliche Bilanzierung which means holistic balancing [9]. The software currently has over 9000 profiles of accurate data coming from such databases as the complete European Life Cycle Database (ELCD) [10], U.S. LCI database from NREL [11], data from trade associations and over 550 Environmental Product Declarations (EPDs) [12]. The GaBi Professional software supports LCA, LCC, Life Cycle Reporting (LCR) and Life Cycle Working Environment (LCWE) [9]. The GaBi software supports the collection and organisation of data as well as the presentation of results. It automatically tracks the material, energy, and emission flows in addition to monetary values (for LCC), working time, and social issues to provide immediate performance accounting in several environmental impact categories [7].

1.6 Lithium-Sulphur Batteries

In the world of energy storage, specifically battery technology, Li-S batteries have emerged as quite promising due to the replacement of sulphur for the metals in the cathode of typical Li-ion batteries. Sulphur is one of the most abundant elements on earth and due to it being an electrochemically active material that can accept up to two electrons per atom at 2,1 V versus Li/Li⁺, sulphur cathode materials have a very high theoretical capacity of 1672 mAh/g [13]. Consequently, Li-S batteries have a theoretical energy density of around 2600 Wh/kg, an entire magnitude of order higher than typical Li-ion batteries [14].

1.6.1 Overview

Li-S batteries were introduced in the late 1960s when the first configuration was presented. This configuration had the positive electrode comprised of elemental sulphur, electronic conductors (carbon or metal powder), and binders, the negative electrode comprised of metallic lithium, and an organic electrolyte separating the two electrodes. This set the base for which Li-S batteries are configured today, typically having a lithium metal anode, an organic liquid electrolyte, and a sulphur composite cathode. The overall redox couple is described by the reaction 1.1 below [13]:



A scheme of the Li-S cell can be seen on the next page in Figure 1.3.

There are three steps in the discharge of the Li-S cell in an organic electrolyte. First through the reaction of $\text{S}^0 \longleftrightarrow \text{S}^{0,5-}$, the sulphur is reduced through a stepwise sequence of soluble polysulphide ions to form S_4^{2-} . Then the insoluble Li_2S_2 is formed by the reaction of $\text{S}^{0,5-} \longleftrightarrow \text{S}^{1-}$. Finally the last step is the interconversion of Li_2S_2 to Li_2S [13].

One drawback of using sulphur as a battery component that must be resolved is the polysulphide shuttle effect, where polysulphide species dissolve in the electrolyte during the charge-discharge process. The dissolution of S_8 into soluble lithium polysulphides Li_2S_x (where x is between 3 and 8) and insoluble sulphides Li_2S_2 and Li_2S result in active material loss, poor cycle life, and low efficiency of the

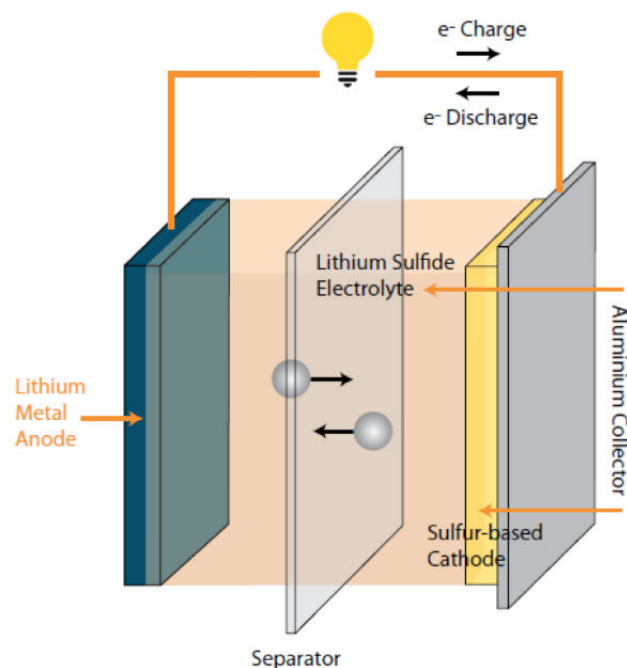


Figure 1.3: A scheme of the Li-S cell displaying the lithium metal anode, sulphur-based cathode, separator, and electrolyte [15].

battery [16]. One solution researched has been to use a liquid electrolyte containing lithium salts such as Lithium bis(trifluoromethanesulphonyl)imide (LiTFSI). Additionally, carbon-based sulphur composites have been researched for the cathode to decrease the polysulphide shuttle effect. Multiwalled carbon nanotubes (MWCNT) have also been shown to be a solution to increase the cycle performance by depositing the sulphur into these nanotubes [14]. Li-S batteries remain a very promising technology but are still far from commercialisation and thus much research has been dedicated globally to its development.

1.6.2 Comparison with Li-ion Batteries

In addition to the higher theoretical capacity and energy density, Li-S batteries are supposed to be more environmentally and economically sustainable than Li-ion batteries (given they have good performance). Sulphur replaces toxic transition metals found in the cathodes of Li-ion batteries such as cobalt and manganese, and sulphur is cheaper and more abundant than these heavy metals [14]. If Li-S batteries can eventually attain higher performance than Li-ion batteries, then this also translates to the batteries lasting longer and less material being wasted in the long run. Table 1.1 below shows a summary of the comparison of these four parameters between Li-S and Li-ion batteries.

Table 1.1: Comparison between Li-S and Li-ion Batteries [13][14][17][18][19][20].

Parameter	Li-S Battery	Li-ion Battery
Theoretical Capacity [mAh/g]	1672	250 - 350
Theoretical Energy Density [Wh/kg]	2600	~ 800
Environmental Impact [heavy metals]	-	Mn, Co, Ni, Fe
Economic Impact [cost of cathode material - \$/kg]	0,12	13,23 - 23,04

As can be seen, in addition to the order of magnitude difference between the two batteries in theoretical capacity and energy density, the environmental impact of the Li-ion battery is much higher due to the heavy metals that the cathodes are composed of (manganese in LMO batteries, nickel and cobalt in NCM batteries, and iron in LFP batteries). The economic impact is also a large point of difference between Li-S and Li-ion batteries: Li-S batteries could theoretically be 110 times cheaper (compared with LMO batteries) or even almost 200 times cheaper (compared with NCM batteries). Thus, Li-S batteries show huge potential in performance and savings in comparison to traditional batteries used in EVs today.

1.7 Literature Research

While there have been many LCAs performed on various types of Li-ion batteries, Li-S batteries are a new technology and since they are not yet commercialised, LCA studies are lacking. The first article on performing a LCA on a Li-S battery was just published this past March, 2017 [2]. A hybrid LCA model was developed for a Li-S battery pack using a lithium metal anode, graphene-sulphur cathode, and LiTFSI electrolyte for the final application in EVs. The battery cell manufacturing processes were modelled with real data collected from an industrial partner's pilot scale production facilities while the synthesis of the graphene-sulphur cathode was modelled from the authors' lab-scale fabrication process [2].

The ReCiPe method was used to perform the LCA; this methodology was developed by several partners in the Netherlands to be able to transform a long list of LCI results into a limited number of indicator scores [21]. Deng, et. al. performed a LCA comparison of their Li-S battery with a conventional lithium-ion battery pack of a Lithium-Nickel-Cobalt-Manganese oxide cathode and a graphite anode (NCM-Graphite). The technical parameters of each battery were dictated as 220 Wh/kg energy density for the Li-S battery and 120 Wh/kg for the NCM-Graphite battery, as well as a mass of 279 kg for the Li-S battery and 531 kg for the NCM-Graphite battery [2]. Thus, in this study the Li-S battery shows superior performance at a decreased mass - both showing that Li-S batteries have the potential to become the new technology in the energy storage world.

The study found that the Li-S battery was more environmentally friendly than the NCM-Graphite battery by 9% up to 90% in the various impact categories. The production of the Li-S battery generates 18.4% lower greenhouse gas (GHG) emissions than the NCM-Graphite battery production. Overall a 9% life cycle GHG emission reduction could be achieved by using Li-S batteries over NCM-Graphite batteries. Additionally, using Li-S batteries over the conventional NCM-Graphite batteries could result in 80-90% reductions in impact categories such as freshwater aquatic ecotoxicity potential (FAETP), marine aquatic ecotoxicity potential (MAETP), terrestrial ecotoxicity potential (TETP), and human toxicity potential (HTP). These reductions were mainly attributed to the fact that the Li-S battery does not use heavy metals such as nickel, cobalt, and manganese and uses much less copper than the NCM-Graphite battery [2].

When it comes to just the Li-S battery production, the cathode was found to take a 7-23% share in most impact categories although it was the main impact source of the metal depletion potential (MDP)

category at 48%; this confirmed the fact that the fabrication of the cathode involves the majority of mass inputs in the battery production. The electrolyte was found to have an approximately 21% share in most impact categories except for marine eutrophication potential (MEP) and ozone depletion potential (ODP) where it accounted for over 85% of these categories most likely due to the synthesis of dimethyl ether (DME) which causes a high amount of ammonia and nitrate emissions. The anode, cell casing, and module packaging were the main contributors to the FAETP, HTP, MAETP, and TETP impact categories. This was found to be due to the copper used for the current collectors and terminals, and the aluminium used in the module packaging [2].

When it comes down to life cycle phases, the production of the battery was found to have a 28% share of the GWP impact while the use phase was found to have a 70% share of the GWP. However, the production had the majority impact in the FAETP, MAETP, TETP, ODP, and HTP categories. Since the use phase entails only the electricity grid, this will vary greatly depending on location; this study was performed in the U.S. (where the electricity impact will also vary by state) thus the use phase may have a higher impact here than in other parts of the world where more renewable energies are used for electricity production [2]. Deng, et. al. provided a decent first LCA study on Li-S batteries and hopefully out of this investigation, more literature will be published in this field.

Another novel type of battery technology currently being researched is the sodium ion (Na-ion) battery. A LCA performed on these types of batteries by Peters, et. al. provided some aid in modelling a LCA on a Li-S battery [22]. The cathode of the Na-ion battery contains similar materials to the Li-S battery such as carbon black and the various binders of styrene-butadiene-rubber (SBR), carboxymethyl cellulose (CMC), and polyvinylidene fluoride (PVDF). The electrolyte is simply NaF_6P instead of LiF_6P in the Li-S battery. The energy density of the Na-ion battery cell being analysed is 128 Wh/kg, so much lower than the energy density of Li-S batteries but with the advantage of not using lithium in the battery which has high environmental and cost impacts [22].

Peters, et. al. found that in the case of Na-ion batteries, the anode provides the highest contribution to GWP impact at 24% in battery production. This is explained by the carbon preparation where sugar is produced from sugar beet and this process is associated with high GHG emissions; additionally the aluminium collector foil in the anode and the nitrogen gas in the carbon production process contribute significantly to this GWP impact. The cathode production is responsible for 20% of the total GWP impact, of which almost half is due to the PVDF binder, the production of which is highly GHG intensive [22]. Whereas metals contribute to the high impacts of Li-ion and Li-S batteries, the carbon production in the Na-ion batteries is what is primarily to blame for the high impact since these batteries don't use most of the metals that Li-ion and Li-S batteries contain. Since Na-ion batteries are still in an early phase like Li-S batteries, LCA research in this field provides a good point of comparison since the batteries are still undergoing investigation into the most sustainable materials and processes used.

While copious LCA literature can be found on various types of Li-ion batteries used in EVs, there is still a severe lack of LCAs performed on up-and-coming batteries such as Li-S, which are currently being researched globally. Through this study, the goal is to add more research to the repertoire and gain more attention for Li-S batteries in the world of EVs.

Chapter 2

Implementation

This section details the goal and scope definition of the LCA, including the objectives, definition of the system, system boundaries, functional unit, impact categories selected, limitations, and assumptions. Then the materials inventory for the two battery cells investigated are given in Section 2.2 along with the parameters of the battery cells in Section 2.3. A description of how the systems were equated for comparison is gone through in Section 2.4 with the new inventory of the IREC cell, battery pack inventory (Section 2.4.1), and the parameters of the battery systems (Section 2.4.2). Finally, calculations for the use phase of the LCA are gone through in Section 2.5.

2.1 Goal and Scope

As described in Section 1.4.1 and per the first main step of the LCA methodology according to ISO 14044, the goal should lay out the purpose of the study and if the LCA results are meant to be used for comparative reasons. The scope involves the characterisation of the system and defines the limitations and assumptions made in the study.

2.1.1 Purpose

This study has two main purposes. The first is to analyse the environmental impacts due to the production of the coin cells from IREC and the cells from the HELIS project. As a second purpose, after an adequate scaling to make both devices equivalent, the cells themselves can be compared; the different ways of manufacturing Li-S battery cells are compared to find the optimal type, chemistry, and materials of the cells that maintain high performance and are as environmentally sustainable as possible. In order to withdraw more conclusions about each battery according to the mentioned purposes, several sensitivity analyses are performed.

2.1.2 Definition of the System

The system in this analysis will depend on the objective since there are two laid out in this study. In the first objective, the system only consists of the cell of the battery; this is what is manufactured currently and the impacts of the process to make just the cell are an important aspect of the study. Then for the second objective, the battery pack is included to be able to compare the two battery cells within the context of a larger application. The pack includes the circuit board (PCB) and battery casing but does not include the full battery management system (BMS) which includes the cooling technology needed. The inventory for the battery packs was taken from literature and ratios of the materials were determined based on the performance and parameters of the cells. Research is currently ongoing on the development of a BMS for these cells.

2.1.3 System Boundaries

The system boundaries also depend on the objective. For the first objective, the LCA is performed using the cradle to gate approach, so from the raw material extraction to the production of the battery cells to find the impacts of the individual cells. Then, to compare the two cells, the cradle to grave approach will be taken for the battery systems, analysing the entire life cycle of the battery, from raw material extraction through production and use of the battery in an EV and finally EOL.

2.1.4 Functional Unit

There are two functional units used here for the two objectives of the study. For the analysis of the impact of one cell, the functional unit used is one Li-S battery cell. For the comparison of the two cells in the cradle to grave approach, the functional unit used is a 22 kWh Li-S battery system that runs 1000 cycles which would carry out around 150.000 km. The two battery systems were scaled to this metric, determining the number of cells and battery packs needed to fulfil the 1000 cycles. The reason for the different functional units is because in the first objective of the study, the impact of one cell is determined and thus, it makes the most sense to have the functional unit be that one cell. However, when comparing the two cells, it is desired to do so based on performance as well, and this is why the functional unit is thus related to the vehicle and not just the battery cell itself.

2.1.5 Selection of the Impact Categories

The CML 2001 method was used to evaluate the impact categories in the GaBi Professional software. This impact assessment method was developed by Leiden University's Institute of Environmental Sciences in Leiden, The Netherlands. CML 2001 limits uncertainties by restricting quantitative modelling to early stages in the cause-effect chain [23]. Eleven different impacts were assessed, displayed in Table 2.1 on the next page with their abbreviations that will be used henceforth and their measurement parameters.

Table 2.1: The eleven different impacts assessed in this LCA.

Impact	Abbreviation	Measurement
Global Warming Potential	GWP	kg CO ₂ -equivalent
Abiotic Depletion	ADP	MJ
Acidification Potential	AP	kg SO ₂ -equivalent
Eutrophication Potential	EP	kg PO ₄ -equivalent
Freshwater Aquatic Ecotoxicity Potential	FAETP	kg DCB-equivalent
Human Toxicity Potential	HTP	kg DCB-equivalent
Marine Aquatic Ecotoxicity Potential	MAETP	kg DCB-equivalent
Ozone Layer Depletion Potential	ODP	kg CFC 11-equivalent
Photochemical Ozone Creation Potential	POCP	kg C ₂ H ₄ -equivalent
Terrestrial Ecotoxicity Potential	TETP	kg DCB-equivalent
Primary Energy Demand	PED	MJ

2.1.6 Limitations

Various limitations were present in this study, most of which were due to lack of sufficient data.

Data was provided for the HELIS project cells in the form of an Excel file listing all the various inputs for the GaBi software. Unfortunately, no processes were explained in detail and thus energy inputs were entered as they were given, rather than knowing exactly where these inputs came from. So while an accurate estimation of the energy consumption in the production of the IREC cells was possible since there was access to the machinery and all details of the processes used, this same detail in data was unavailable for the HELIS cells.

Since only the battery cells are being researched thus far, no data was provided on the battery pack for the overall system and likewise, no current methods of recycling or waste disposal exist for these types of batteries.

Finally, not all data was available for providers of the materials used in the batteries, especially for the HELIS batteries. To be able to include this transport data in the LCA, many assumptions were made which are outlined in the next section.

2.1.7 Main Assumptions

Based on these various limitations described above in Section 2.1.6, assumptions were deduced to attempt to provide the best outcome for the study.

For the energy consumption of the cell production, it was assumed that the values provided from the HELIS data were on an industrial scale since the values were quite low. Thus, the energy consumption calculated for the IREC coin cells (see Section 2.2.2) is assumed for an industrialised process, thus producing material for many more cells than are currently produced. This gave energy inputs on a similar scale for both cells; otherwise the energy consumption of the IREC cells would produce results giving IREC cells a much larger environmental impact than the HELIS cells. However, for the IREC

cylindrical cells used in the battery system (see Section 2.4), where the surface area of the electrodes is much greater than for the coin cells, the energy consumption calculated had to be assumed for only one cylindrical cell at a time. Since this is not optimal, a sensitivity analysis on this energy consumption was performed in Section 3.3.2 where the energy consumption was decreased to industrial levels (which is not yet possible in the IREC labs).

Since Li-S batteries are still in research, data concerning EOL is yet to be established. Thus the approach of open-loop recycling has been chosen; this means that the recycling processes are not accounted for as they are allocated in the life cycle of the future product that is produced from the recycled material. The analysis then reflects the benefit of using a material that can be and is recycled and no environmental burdens are allocated in that case [24]. Figure 2.1 below displays a schematic of the open-loop recycling methodology.

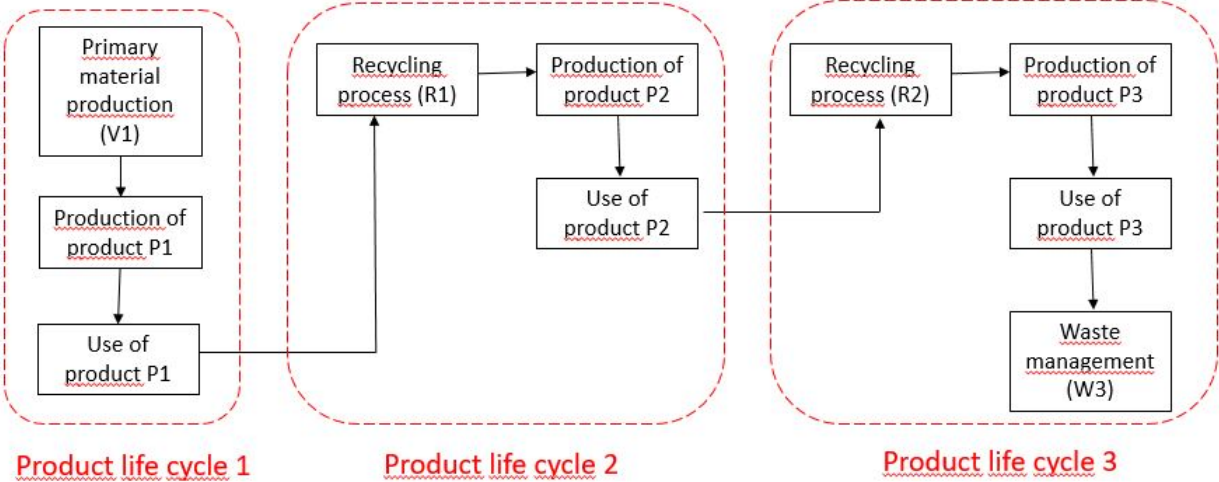


Figure 2.1: Schematic displaying the methodology of open-loop recycling [24].

This schematic shows that all material in product 1 is recycled into product 2 and all material in product 2 is recycled into product 3. Product 2 and product 3 are produced from this recycled material only (no primary materials go into their production). However, the material from product 3 is not recycled after use and goes to waste management. In the LCA models created for this study, all of the product life cycle 2 and product life cycle 3 are considered as waste management in the end of life phase.

For the EOL phase of the life cycle, it was assumed that metals and plastics not coming into contact with hazardous materials could be recycled (e.g. casing materials), and anything within the electrodes and other parts that contained a hazardous material would be considered as hazardous as well.

Finally, almost all transportation in the LCA was assumed due to not having sufficient data. For the shipment of materials for production purposes, providers were researched and the most appropriate transport was chosen for these shipments. In the HELIS project, shipment of cell parts between partners of the project were also estimated to find the most appropriate modes of transport. In the EOL phase, the transport of materials to a sorting facility was estimated at 500 km and the transport of the recycled materials to a recycling facility was estimated at 200 km. These were most likely overestimations, to be

sure that the transportation impact was covered as appropriately as possible.

Assumptions for System Comparison

When it came to sizing the battery systems for comparison, there was a lack of data since only data on the cells was provided and not the battery systems that they would be scaled to. Characteristics such as battery efficiency, new battery energy density, and accurate battery casing information were not provided and thus this study was accommodated accordingly. Data from literature was used for the sizing of the battery system. The LCA study on Li-S batteries that Deng, et. al. [2] performed was used as a guideline in the sizing of the battery system. Additionally, since the battery efficiency was unknown, a rudimentary approach was taken to calculate the electricity usage in the charging of the battery.

2.2 Life Cycle Inventory

This section includes a comprehensive inventory of the materials used in the two different cells - the second main step of the LCA methodology according to ISO 14040 (Section 1.4.2). While some parts of the cells are the same, most components of the cells are quite different. Additionally, the characteristics of the two cells are given, including cell weight, gravimetric energy density, and cycle life.

The process flows made in GaBi are included in the appendices of this report. Appendix A contains all the GaBi process flows for the HELIS battery and Appendix B contains all the GaBi process flows for the IREC battery.

2.2.1 HELIS Cells

A complete inventory of the materials used in the HELIS battery cell is given in Table 2.2 along with their weight in grams, their weight ratio (% of total weight), and any comments deemed necessary. As can be seen it is a typical Li-S cylindrical cell with a sulphur-carbon composite cathode and lithium metal anode. It uses a cathode binder, two of which were tested here: the first one is styrene-butadiene-rubber (SBR) and carboxymethyl cellulose (CMC) in water and the second one is polyvinylidene fluoride (PVDF) in N-methyl-2-pyrrolidone (NMP). PVDF is not in the GaBi or Ecoinvent databases and thus polyvinyl fluoride (PVF) from the Ecoinvent database was used instead as this was the closest material to PVDF available in the databases accessible. A sensitivity analysis was performed on these two binders in Section 3.3.3 to see which is more sustainable. The electrolyte is a tetraethylene glycol dimethyl ether (TEGDME, also known as tetraglyme)/dioxane mix; since TEGDME is not in the GaBi or Ecoinvent databases, ethylene glycol dimethyl ether (also known as glyme) was used instead since they are produced by the same reaction route. The cell materials also include a polypropylene separator, a cathode connect and anode connect, and a Al-PET-PP composite cell casing [25]. Photos of the cells were taken after production and before testing, displayed in Figure 2.2 on the next page.



Figure 2.2: Photos of the first prototype HELIS cells.

Table 2.2: Material inventory for the HELIS battery cell [25].

CONFIDENTIAL

2.2.2 IREC Coin Cells

A complete inventory of the materials used in the IREC battery cell is given in Table 2.3 along with their weight in grams, their weight ratio (% of total weight), and any comments deemed necessary. In contrast to the HELIS battery cell which is cylindrical, the IREC Li-S cells are coin cells with a sulphur-carbon composite and lithium metal anode, however the carbon composite is produced in house by way of carbon nanofibers that endure a long, energy-intensive process. Additionally, these cells differ in the casing, which is all stainless steel, provided by a coin cell part manufacturer in Japan [26]. The electrolyte used is the same as in the HELIS cells and the separator is again a membrane made from PP. Apart from the standard electrodes, electrolyte, separator, and casing, these cells also contain additional parts since they are coin cells: a gasket made from PP, a spacer made from stainless steel, and a spring made from stainless steel so that the coin cell can be pressed by a crimping machine to the same measurements every time [27]. Photos of the cells were taken after production and before testing, displayed in Figure 2.3 below.



Figure 2.3: Photos of the cells manufactured by IREC (left) and their parts (right).

Table 2.3: Material inventory for the IREC battery cell [27].

CONFIDENTIAL

2.3 Parameters

The parameters of both cells are given below in Table 2.4, including gravimetric energy density. As can be seen, they are two very different cells made for different applications. One is a cylindrical cell made for mobile applications such as EVs while the other is a coin cell made for stationary applications. Thus, on this scale they are not comparable.

Table 2.4: Parameters of the two battery cells [25][27].

Parameter	HELIS Battery Cell	IREC Battery Cell
Gravimetric energy density (Wh/kg)	266	1050
Mass of cell (g)	290,56	3,53

The reason for the difference in target number of cycles is due to the fact that they are two different battery cells. Coin cells are very small devices that will not perform as many cycles as cylindrical or pouch cells and this is another reason why they are not appropriate for high-intensity use applications such as electric vehicles.

2.4 Equivalency for Comparison

To be able to compare the two battery cells, they were sized up to battery systems that could be used in EVs: 22 kWh battery systems that would run 1000 cycles, allowing an EV to travel approximately 150.000 km over its lifetime. The battery system was chosen to be 22 kWh since it is a median power for modern EVs and is the power for the BMW i3 battery system (for reference, the Toyota Prius uses a 4,4 kWh battery pack, the Chevy Volt uses a 16 kWh battery pack, the Nissan Leaf uses a 30 kWh battery pack, and the Tesla Model S uses a 60 kWh battery pack) [28].

To be able to compare the two cells for EV application, they had to both be in cylindrical form (or pouch form, but since the HELIS cell is already in cylindrical form, this makes the most sense). Coin cells are not used in EV applications since they are too small and a huge amount of them would be needed in the battery pack. Thus, the chemistry of the IREC cell was taken and used in a cylindrical cell. The electrodes, electrolyte, and membrane were scaled up to have the same weight as these same parts in the HELIS cylindrical cell but still having the same ratio of weight as in the IREC coin cell. The parts pertaining to the coin cell were removed (gasket, spacer, and spring) and were replaced with the electrode connects used in the HELIS cell. The cell casing from the HELIS cell was used for the IREC cylindrical cell since they will be the same form and weight (just differing chemistry). The materials inventory for the IREC cylindrical battery cell is given in Table 2.5 to show the differences more clearly.

Table 2.5: Material inventory for the IREC cylindrical cell [27].

CONFIDENTIAL

To determine the number of cells needed for each battery system, the gravimetric energy density was

used to find the energy density per cell and then the energy density per cell was used to find the number of cells required to have a 22 kWh battery system. Table 2.6 on the next page gives the parameters used in these calculations to show clearly how the number of cells was determined, along with the total mass of the cells in one battery.

Table 2.6: Parameters used in the calculation of the number of cells in a battery.

Parameter	HELIS	IREC
Gravimetric energy density (Wh/kg)	266	1050
Mass of cell (g)	290,56	286,55
Energy density per cell (Wh/cell)	77	301
Number of cells needed for a 22 kWh system	284,6	73,1
Total mass of cells in one battery (kg)	82,71	20,95

2.4.1 Battery Pack

Battery pack inventory was taken from literature since battery packs are not currently being manufactured by IREC or for the HELIS project. Table 2.7 below shows the inventory for the battery pack with the respective weights for the HELIS battery and IREC battery. To find the total weight of the battery pack, the weight ratio of cells to total battery was taken from literature (specifically Deng, et. al. since they also performed a LCA on Li-S batteries so this seemed the most appropriate data to use) [2]. Then, the software BatPac was used to determine the weight ratios of the battery pack materials [29].

Table 2.7: Material inventory for the battery pack for the two battery systems [29].

Material	HELIS Weight (kg)	IREC Weight (kg)
Battery Pack	42,70	10,82
Stainless steel	27,29	6,91
Aluminium foil	8,91	2,26
Aluminium extrusion profile	3,83	0,97
Printed wiring board	2,62	0,66
Copper	0,046	0,012
Copper sheet	5,75E-04	1,46E-04

2.4.2 Equivalency Parameters

A summation of the mass of the cells for each battery and the mass of the battery pack results in the total mass of the battery system which is given in Table 2.8 below. The table also summarises the characteristics of the battery systems.

Table 2.8: Parameters of the equivalency of the two batteries.

Parameter	HELIS Battery	IREC Battery
Mass of cells (kg)	82,71	20,95
Mass of battery pack (kg)	42,70	10,82
Total mass of battery system (kg)	125,41	31,77
Gravimetric energy density (Wh/kg)	266	1050

The energy density of the IREC cell, going from a coin cell to a cylindrical form, will most certainly decrease. However, this being a theoretical study in that this cylindrical cell does not yet exist, the energy density was left as is and a sensitivity analysis was performed with varying energy densities, which can be found in Section 3.3.1.

Additionally, in regards to cycle life, since these battery cells are still in the research phase and not achieving the target number of cycles, to simplify the comparison, the cycle life was set at 1000 for both batteries. For a total driving distance of 150.000 km over the lifetime of the vehicle, 1000 cycles is an average cycle life for the EV battery. Thus, the results presented and interpreted in Section 3.2 are of theoretical future battery systems.

2.5 Use Phase

The process of calculating the electricity consumption for the use phase in the LCA had to be simplified due to the lack of data on the battery systems that were composed (battery efficiency as well as discharged energy are unknown). Thus, a fuel consumption rate was taken from literature. The value of 0,586 MJ/km was used since this was used in the LCA of Li-S batteries [30]. This seems an appropriate value to take since there is a range in literature from 0,48 MJ/km to 0,623 MJ/km [31]. In fact, the electricity consumption is most likely very conservative since the Li-S batteries studied in the LCA published had an energy of 61,3 kWh and in this study the batteries are set to 22 kWh [2]. The electricity mix used was the average European (EU-28) mix, shown below in Figure 2.4.

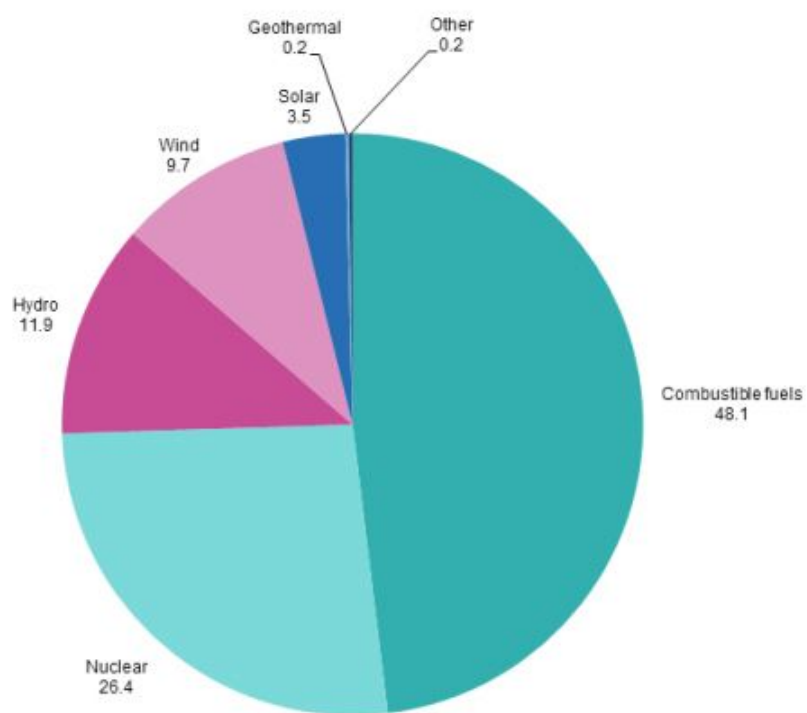


Figure 2.4: The EU-28 electricity mix as of 2015 (% of total, based on GWh) [32].

Chapter 3

Results

In this section the Life Cycle Impact Assessment (LCIA) and interpretation is presented first for the battery cells (first objective) in Section 3.1 and after for the battery systems (second objective) in Section 3.2. The way the LCIA is presented is that first, tables of all the impact results are given and then certain impact categories are gone into more detail afterwards. The larger impacts are given in bold to highlight from what parts of the battery/what phase of life contribute the most to the impact categories. The results of three sensitivity analyses are then displayed and interpreted in Section 3.3. In the sensitivity analysis results, the smaller impacts are given in bold to highlight which option is the most sustainable.

3.1 Life Cycle Impact Assessment and Interpretation for Cradle to Gate Analysis

Here the results are presented and interpreted for the first objective of this study: the production of one battery cell (a cradle to gate analysis). First the results are given for the HELIS battery cell in Section 3.1.1 and then the results are given for the IREC battery cell in Section 3.1.2 to see which parts of the cells have the highest impacts and which impact categories have the most negative effects.

3.1.1 HELIS Cell

The LCIA results for the cradle to gate analysis of the HELIS battery cell (solely cell production) are shown in Table 3.1 where they are categorised by stream (primary materials, production, and transport) and afterwards again in Table 3.2 where they are categorised by cell part (cathode, anode, electrolyte, etc.). As can be seen in Table 3.1, the extraction and refinery of the primary materials contribute essentially completely to all the impact categories, ranging from 90% (such as in ADP) all the way up to 99,9% (in HTP, TETP, and ODP). It is possible that the data provided on these cells did not account for all production methods, and thus the production does not seem to account for almost any impact. However, the transport having such a small effect is surprising since there is quite a bit of transport between all the partners. This will be a theme among the results, that the transport has negligible effects on the impact

categories. Despite transport seeming to be a very unsustainable part of the process of production of a product, in reality the primary materials extraction and refinery outshines it completely when it comes to environmental impacts.

Table 3.1: LCIA results for the HELIS battery cell (cradle to gate analysis) categorised by stream.

Impact Category	Total	Primary Materials	Production	Transport
GWP [kg CO ₂ -eq.]	3,74E+00	3,44E+00	6,90E-02	2,39E-01
ADP [MJ]	4,69E+01	4,26E+01	8,84E-01	3,32E+00
AP [kg SO ₂ -eq.]	1,94E-02	1,85E-02	1,34E-04	7,05E-04
EP [kg PO ₄ -eq.]	8,27E-03	8,10E-03	1,34E-05	1,54E-04
HTP [kg DCB-eq.]	5,35E+00	5,34E+00	2,35E-03	8,44E-03
FAETP [kg DCB-eq.]	1,03E+00	1,02E+00	1,24E-04	1,23E-03
MAETP [kg DCB-eq.]	5,30E+03	5,29E+03	4,78E+00	3,04E+00
TETP [kg DCB-eq.]	2,31E-02	2,31E-02	3,02E-05	3,58E-05
ODP [kg CFC 11-eq.]	2,96E-07	2,96E-07	1,86E-12	3,37E-13
POCP [kg C ₂ H ₄ -eq.]	1,21E-03	1,16E-03	1,09E-05	4,36E-05
PED [MJ]	5,98E+01	5,50E+01	1,48E+00	3,35E+00

From Table 3.2 below, the part of the cell production which contributes most to the impact categories can be seen. The anode (lithium metal) has the majority effect on all impact categories except for human toxicity where the cathode and electrolyte share the effects with the anode. In the rest of the impact categories though, the anode ranges from having 51% contribution to abiotic depletion and primary energy up to 92% contribution to ozone layer depletion potential. This is due to the fact that lithium metal is a very highly intensive metal to extract and refine for use in products.

Table 3.2: LCIA results for the HELIS battery cell (cradle to gate analysis) categorised by cell part.

Impact Category	Total	Cathode	Anode	Electrolyte	Separator	Casing
GWP [kg CO ₂ -eq.]	3,74E+00	5,69E-01	2,36E+00	3,29E-01	1,21E-01	2,20E-01
ADP [MJ]	4,69E+01	9,17E+00	2,39E+01	6,75E+00	2,37E+00	2,68E+00
AP [kg SO ₂ -eq.]	1,94E-02	2,28E-03	1,35E-02	1,67E-03	4,62E-04	1,01E-03
EP [kg PO ₄ -eq.]	8,27E-03	1,70E-04	7,35E-03	5,49E-04	6,49E-05	6,37E-05
HTP [kg DCB-eq.]	5,35E+00	1,60E+00	1,48E+00	1,38E+00	5,31E-03	8,84E-01
FAETP [kg DCB-eq.]	1,03E+00	5,07E-03	9,24E-01	9,38E-02	5,19E-04	1,44E-03
MAETP [kg DCB-eq.]	5,30E+03	7,87E+02	3,30E+03	7,68E+02	5,08E+00	4,32E+02
TETP [kg DCB-eq.]	2,31E-02	1,09E-03	1,92E-02	1,98E-03	9,60E-06	7,36E-04
ODP [kg CFC 11-eq.]	2,96E-07	5,12E-10	2,74E-07	2,22E-08	3,02E-13	2,42E-12
POCP [kg C ₂ H ₄ -eq.]	1,21E-03	1,63E-04	7,63E-04	1,52E-04	4,02E-05	6,64E-05
PED [MJ]	5,98E+01	1,21E+01	3,06E+01	7,60E+00	2,55E+00	4,32E+00

Carbon Footprint Analysis

Since the carbon footprint of a product or process is one of the most sought-after impacts, it will be gone into more detail for all analyses. The pie chart given in Figure 3.1 below shows the effects of the cell

parts on the global warming potential in a more visual and clear way. The anode dominates with a 66% contribution, with the cathode next, contributing 16%, and the electrolyte contributing 9%. The casing and separator have the lowest contributions to the GWP. Lithium metal has a value of 59,4 kg CO₂-eq. per kg of material (the majority of which comes from the emission of 53,8 kg CO₂) whereas sulphur has a value of 0,655 kg CO₂-eq. per kg of material (again the majority of which comes from the emission of 0,563 kg CO₂). It can be seen from this almost 100X difference why the anode has such high effects in this impact category.

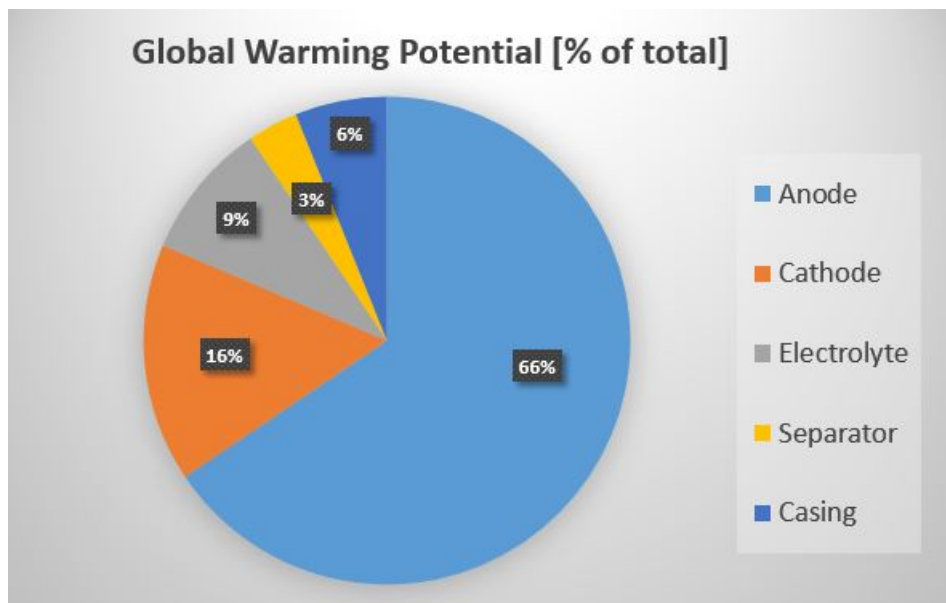


Figure 3.1: Pie chart displaying the contributions of each part of the HELIS cell production to global warming potential in percentages.

Primary Energy Demand

The primary energy demand shows the same trends as the GWP, with the anode having the most contribution at 54%, next the cathode at 21%, and the electrolyte contributing 13%. However, here the anode does have less effect on the primary energy demand, most likely due to the energy needed in producing the cathode. The anode still has the highest effect since lithium metal has a value of 773 MJ per kg of material (the majority of which comes from 266 MJ of hard coal) whereas sulphur has a value of 34,2 MJ per kg of material (the majority of which comes from 29,4 MJ of crude oil), an over 20X difference.

Human Toxicity Potential

The human toxicity potential is where these trends change. As seen in the pie chart in Figure 3.3 below, now the cathode has the dominant contribution at 30% but it has almost equal effects along with the anode and electrolyte at 28% and 26% contributions respectively.

The dominant material in the cathode causing these high impacts is the aluminium. Whereas lithium has a value of 38 kg DCB-eq. per material (the majority of which comes from the emission of chromium

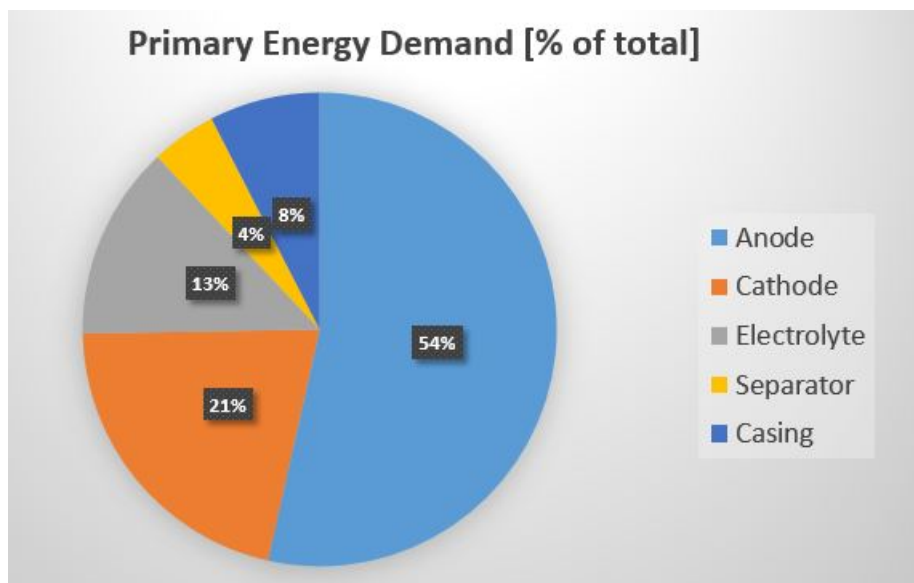


Figure 3.2: Pie chart displaying the contributions of each part of the HELIS cell production to primary energy demand in percentages.

(+VI), selenium, and arsenic), aluminium has a value of 41,5 kg DCB-eq. per kg material (the majority of which comes from the emission of carcinogenic polycyclic aromatic hydrocarbons (PAH). The dominant material in the electrolyte causing its high impacts is the ethylene glycol dimethyl ether. Its value for HTP is 31,6 kg DCB-eq. per kg material (the majority of which comes from the emission of ethylene oxide), and since around the same mass is used for it as the aluminium in the cathode and lithium in the anode (36-38 g), this explains why the cathode, anode, and electrolyte share the dominant effects on human toxicity. Since aluminium and ethylene glycol dimethyl ether are two more materials along with lithium contributing majorly to the environmental impacts of the battery cell, these could be decreased in mass or be replaced with other materials altogether.

3.1.2 IREC Cell

The LCIA results for the cradle to gate analysis of the IREC battery cell (solely cell production) are shown in Table 3.3 where they are categorised by stream (primary materials, production, and transport) and afterwards again in Table 3.4 where they are categorised by cell part (cathode, anode, electrolyte, etc.). As can be seen in Table 3.3, the production here contributes to the majority of all impact categories except for ozone layer depletion potential. It ranges from 57% impact on acidification potential up to 99,5% on TETP. The IREC cells have much more impact coming from the production stream compared with the HELIS cell due to the production of the cathode which is much more intensive. The cathode is made completely from scratch, first making the carbon nanofibers and then heating the nanofibers with sulphur for several hours in a high-power oven [27]. Again the transport has very low effects in comparison to the primary materials and production but here it does have higher effects in some categories than the HELIS cell transport. In ADP, EP, and primary energy, the transport has impacts ranging from 11% to 16%. This would be due to the air transport of the stainless steel coin cell parts from Japan that would

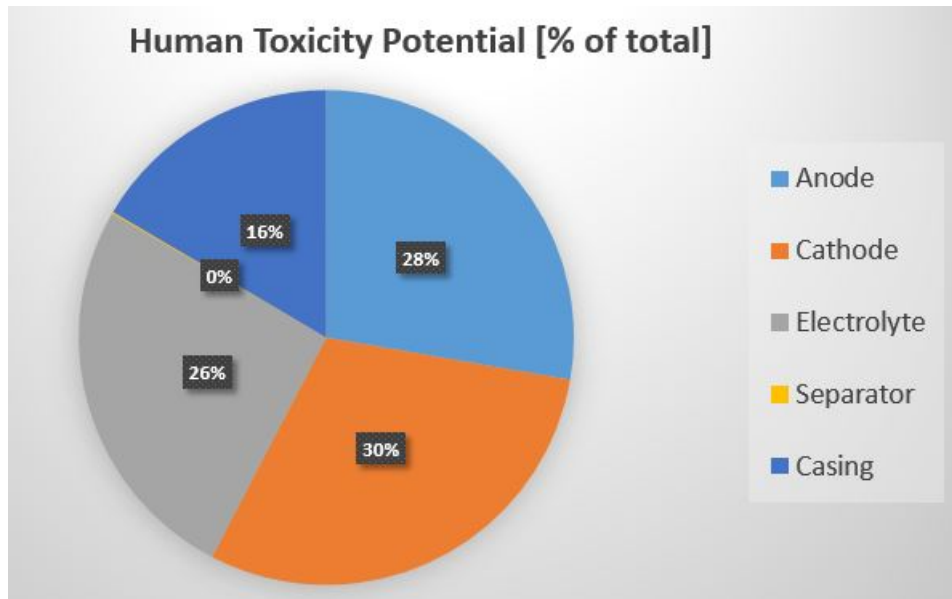


Figure 3.3: Pie chart displaying the contributions of each part of the HELIS cell production to human toxicity potential in percentages.

be much more impactful than the train transport the HELIS cells had involved.

Table 3.3: LCIA results for the IREC battery cell (cradle to gate analysis) categorised by stream.

Impact Category	Total	Primary Materials	Production	Transport
GWP [kg CO ₂ -eq.]	4,89E-01	2,33E-02	4,46E-01	1,99E-02
ADP [MJ]	1,69E+00	2,72E-01	1,14E+00	2,78E-01
AP [kg SO ₂ -eq.]	7,25E-04	2,50E-04	4,10E-04	6,44E-05
EP [kg PO ₄ -eq.]	1,04E-04	1,39E-05	7,73E-05	1,29E-05
HTP [kg DCB-eq.]	1,03E+00	8,81E-02	9,42E-01	3,51E-04
FAETP [kg DCB-eq.]	1,62E-02	7,40E-04	1,54E-02	6,50E-05
MAETP [kg DCB-eq.]	7,69E+02	1,20E+01	7,57E+02	1,61E-01
TETP [kg DCB-eq.]	2,26E-01	1,03E-03	2,25E-01	1,75E-06
ODP [kg CFC 11-eq.]	1,06E-09	1,03E-09	2,50E-11	2,52E-15
POCP [kg C ₂ H ₄ -eq.]	5,69E-05	1,69E-05	3,53E-05	4,65E-06
PED [MJ]	2,50E+00	3,55E-01	1,86E+00	2,79E-01

From Table 3.4 below, the parts of the cell production which contribute most to the impact categories can be seen. Mostly the stainless steel parts - spacer, spring, and casing - have the highest effects on all impact categories except for ODP where the anode has a high impact and primary energy where the cathode has a high impact as well. Steel is highly intensive to create, requiring the extraction and mining of iron and then high heat consumption to smelt the iron. In a coin cell, the use of steel is unavoidable and since it is easily recyclable it is a desirable product to use, but in batteries for use in EVs, the use of steel can be minimised as much as possible.

Table 3.4: LCIA results for the IREC battery cell (cradle to gate analysis) categorised by cell part.

Impact Category	Total	Cathode	Anode	Electrolyte	Separator	Spacer	Spring	Gasket	Casing
GWP [kg CO ₂ -eq.]	4,89E-01	3,29E-02	9,16E-04	1,73E-04	9,89E-06	1,58E-01	1,37E-01	8,59E-04	1,60E-01
ADP [MJ]	1,69E+00	3,79E-01	9,27E-03	3,54E-03	2,54E-04	5,07E-01	2,48E-01	1,61E-02	5,28E-01
AP [kg SO ₂ -eq.]	7,25E-04	8,81E-05	5,32E-06	8,77E-07	4,84E-08	2,50E-04	1,18E-04	2,32E-06	2,61E-04
EP [kg PO ₄ -eq.]	1,04E-04	9,89E-06	2,90E-06	2,88E-07	3,71E-09	3,33E-05	2,30E-05	4,18E-07	3,42E-05
HTP [kg DCB-eq.]	1,03E+00	1,80E-03	5,85E-04	7,19E-04	8,58E-08	3,53E-01	3,17E-01	1,99E-05	3,57E-01
FAETP [kg DCB-eq.]	1,62E-02	8,52E-05	3,64E-04	4,90E-05	3,14E-09	5,28E-03	5,10E-03	3,96E-06	5,31E-03
MAETP [kg DCB-eq.]	7,69E+02	3,02E+00	1,30E+00	4,01E-01	7,07E-04	2,56E+02	2,51E+02	2,11E-02	2,57E+02
TETP [kg DCB-eq.]	2,26E-01	1,78E-05	6,17E-06	1,04E-06	5,54E-10	7,53E-02	7,49E-02	1,49E-07	7,56E-02
ODP [kg CFC 11-eq.]	1,06E-09	2,24E-11	1,08E-10	1,16E-11	5,43E-20	4,22E-10	4,43E-11	1,74E-15	4,51E-10
POCP [kg C ₂ H ₄ -eq.]	5,69E-05	6,29E-06	2,96E-07	7,72E-08	4,39E-09	1,95E-05	1,03E-05	2,00E-07	2,02E-051
PED [MJ]	2,50E+00	1,02E+00	1,19E-02	3,99E-03	2,83E-04	5,72E-01	2,75E-01	1,67E-02	5,96E-01

Carbon Footprint Analysis

The pie chart given in Figure 3.1 below shows the effects of the cell parts on the global warming potential in a more visual and clear way.

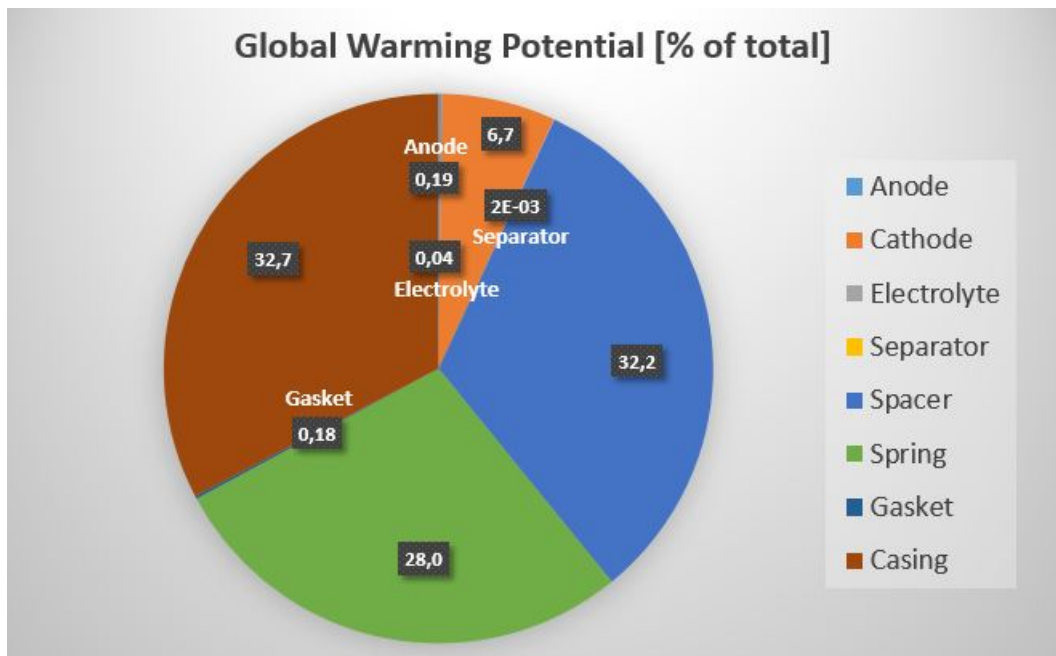


Figure 3.4: Pie chart displaying the contributions of each part of the IREC cell production to global warming potential in percentages.

In contrast to the HELIS cell, the IREC cell has more of a division of the effects among the different parts. The three parts made of stainless steel - spring, spacer, and casing - dominate with 28%, 32,2%, and 32,7% contributions. The cathode is next with a 6,7% contribution. The anode, electrolyte, and separator have the smallest effects. Whereas the anode has an almost 15% weight ratio in the HELIS cell, the anode has a much smaller weight ratio in the IREC cell, due to the dominance of the weight coming from the steel parts, and this is why the anode has such a small effect on the impact categories for the IREC cell. Stainless steel has a value of 3,16E+03 kg CO₂-eq. per kg of material (the majority of which comes from the emission of 2,95E+03 kg CO₂). This is over 50X that of lithium and almost 5000X that of sulphur - so it is quite obvious why the steel parts would have the highest carbon footprint

impacts.

Primary Energy Demand

The primary energy demand has slightly different trends than the carbon footprint. As can be seen in Figure 3.5, the cathode now dominates with a 41% contribution to the primary energy and the casing and spacer coming next with 24% and 23% contributions respectively. This is because the production of the cathode is quite energy-intensive, whereas the other parts do not go through an energy-intensive process to be used in the cell.

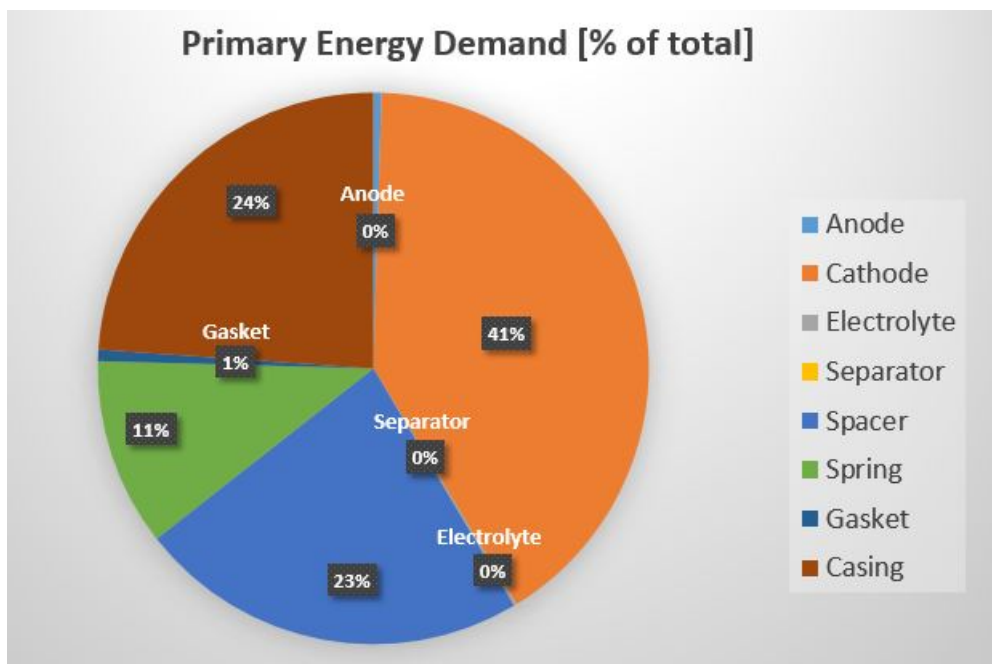


Figure 3.5: Pie chart displaying the contributions of each part of the IREC cell production to primary energy demand in percentages.

Ozone Layer Depletion Potential

The ozone layer depletion potential shows again a different trend than carbon footprint or primary energy demand. Displayed in the pie chart in Figure 3.6, the casing and spacer dominate with 43% and 40% contributions. Next, the anode comes with a 10% contribution and the spring with a 4% contribution. As described earlier, the production dominated every impact category except for ODP where the primary materials dominate, which again is from the stainless steel. It has a value of $2,45E-04$ kg CFC 11-eq. for every kg of material but lithium has a value of $7,03E-06$ kg CFC 11-eq. for every kg of material and sulphur only $2,34E-12$ kg CFC 11-eq. for every kg of material. Thus these differences account for the reason the steel parts dominate this category as well.

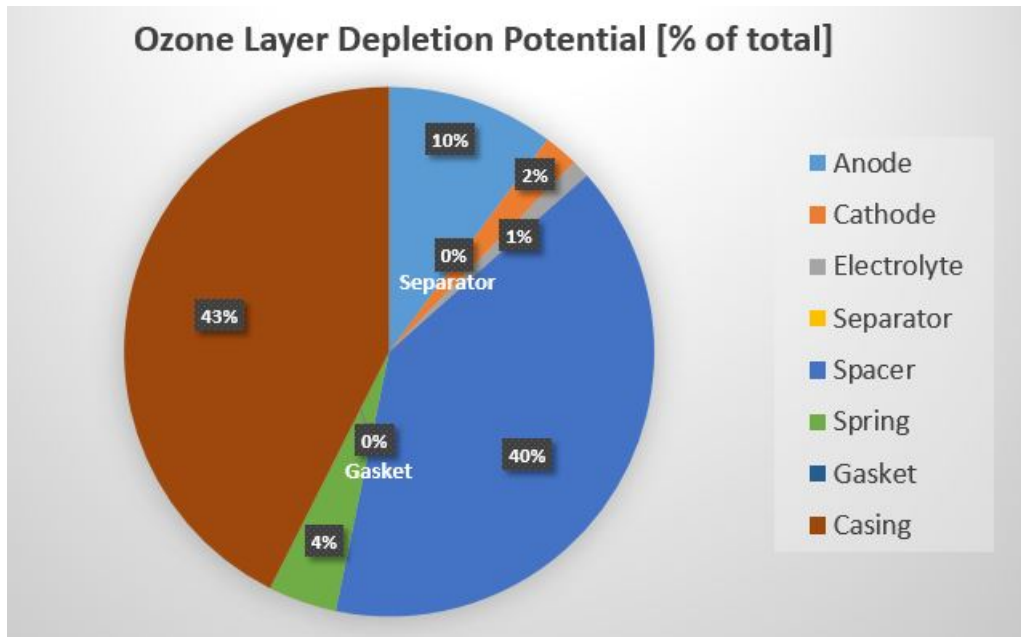


Figure 3.6: Pie chart displaying the contributions of each part of the IREC cell production to ozone depletion potential in percentages.

3.2 Life Cycle Impact Assessment and Interpretation for Cradle to Grave Analysis

Here the results are presented and interpreted for the second objective of this study: the impacts of the entire life cycle of a battery for use in an EV (cradle to grave analysis). First the results are given for the HELIS battery in Section 3.2.1 and then the results are given for the IREC battery in Section 3.2.2 to compare which battery is more sustainable in EV applications in Section 3.2.3.

3.2.1 HELIS Battery

The LCIA results for the cradle to grave analysis of the HELIS battery (from battery production through the use of the battery in an EV all the way to EOL) are shown in Table 3.5 where they are categorised by phase of life. The use phase dominates the GWP, ADP, AP, POCP, and primary energy demand categories while the battery production dominates the EP, HTP, FAETP, MAETP, TETP, and ODP categories. The material extraction for the battery production would have higher effects on the ecotoxicity potentials while electricity production would have a higher effect on carbon footprint due to the amount of electricity consumed over the lifetime of the EV and battery.

Carbon Footprint Analysis

In the pie chart displayed in Figure 3.7 below, it is seen that the use phase contributes the majority to the carbon footprint with the battery production only having a 15% contribution and EOL having a negligible contribution. This is due to the high electricity consumption ($8,74E+04$ MJ) the EV battery uses over its lifetime. But this would most certainly differ in different areas of the world, depending on the electricity

Table 3.5: Impact assessment results for the HELIS battery (cradle to grave analysis) categorised by phase of life.

Impact Category	Total	Battery Production	Use	End of Life
GWP [kg CO ₂ -eq.]	1,28E+04	1,94E+03	1,08E+04	4,75E+01
ADP [MJ]	1,38E+05	2,27E+04	1,15E+05	2,25E+02
AP [kg SO ₂ -eq.]	4,33E+01	1,25E+01	3,08E+01	7,70E-02
EP [kg PO ₄ -eq.]	1,56E+01	1,29E+01	2,79E+00	1,65E-02
HTP [kg DCB-eq.]	6,96E+03	6,45E+03	4,92E+02	7,14E+00
FAETP [kg DCB-eq.]	2,87E+03	2,84E+03	2,16E+01	2,83E-01
MAETP [kg DCB-eq.]	1,05E+07	9,27E+06	1,23E+06	2,34E+03
TETP [kg DCB-eq.]	5,11E+01	2,36E+01	7,62E+00	1,99E+01
ODP [kg CFC 11-eq.]	1,40E-04	1,39E-04	4,79E-07	5,89E-11
POCP [kg C ₂ H ₄ -eq.]	2,75E+00	7,86E-01	1,97E+00	-6,07E-03
PED [MJ]	2,83E+05	2,96E+04	2,53E+05	2,67E+02

mix used. In China, where the electricity mix is heavily dominated by coal, the use phase would have an even higher contribution. But in Sweden, where the electricity mix is dominated by nuclear and hydro, the use phase would have a very small contribution due to the dominance of renewable sources of power.

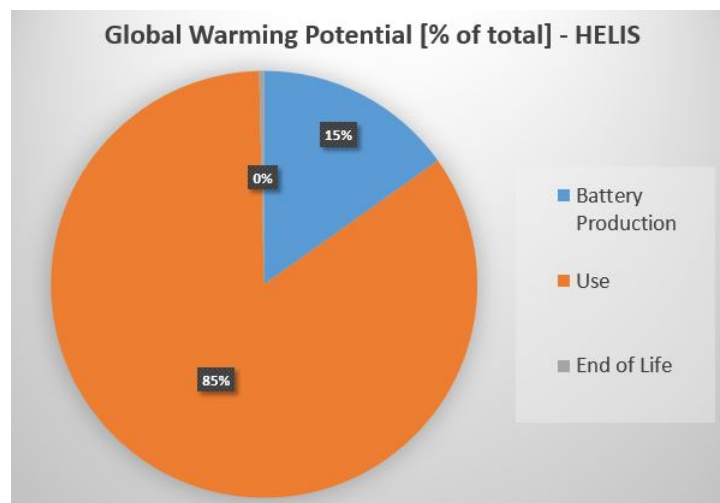


Figure 3.7: Pie chart displaying the contributions of each phase of the life cycle of the HELIS battery to global warming potential in percentages.

Marine Aquatic Ecotoxicity Potential

In contrast to the carbon footprint, the marine aquatic ecotoxicity potential is dominated by the battery production as seen in Figure 3.8 below. The raw material extraction plays a large role in the marine aquatic ecotoxicity potential, with the emissions associated with the production of various materials (steel, lithium, carbon) having high effects on seawater. This is the same for the FAETP, TETP, and HTP.

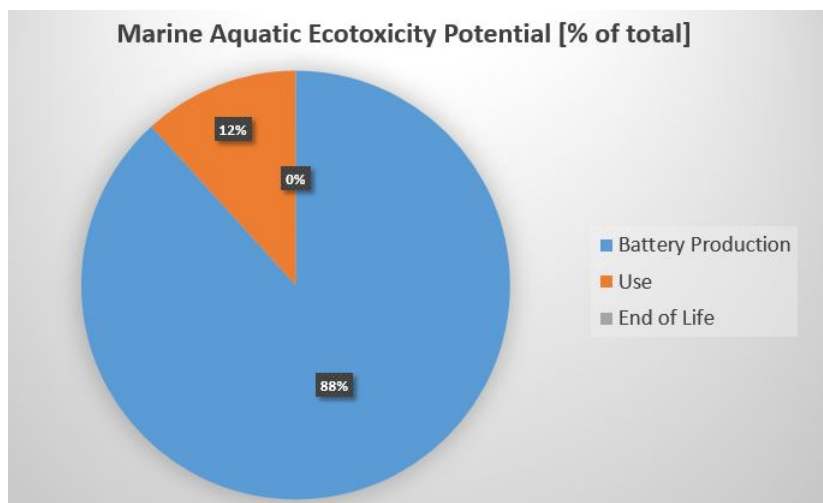


Figure 3.8: Pie chart displaying the contributions of each phase of the life cycle of the HELIS battery to marine aquatic ecotoxicity potential in percentages.

Terrestrial Ecotoxicity Potential

The terrestrial ecotoxicity potential shows different results from either the global warming potential and the marine aquatic ecotoxicity potential. Whereas in the other impact categories, the EOL phase had negligible effects, here the EOL has a very important effect on the TETP, contributing 39%, just after battery production which contributes 46%.

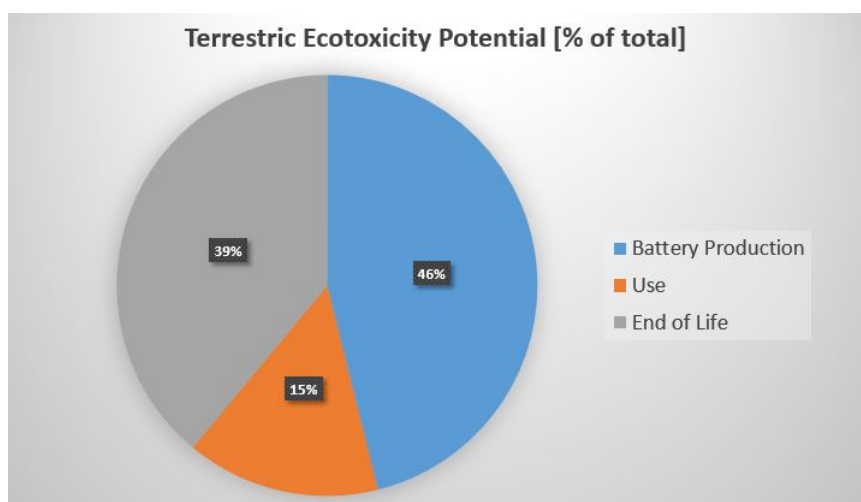


Figure 3.9: Pie chart displaying the contributions of each phase of the life cycle of the HELIS battery to terrestrial ecotoxicity potential in percentages.

This is due to the fact that the hazardous waste treatment has a high impact on the terrestrial ecotoxicity potential. It has a value of 324 kg DCB-eq. per kg of hazardous waste (almost entirely coming from the emission of mercury) whereas the electricity consumption for the use phase has a value of $3,14E-04$ kg DCB-eq. Thus, this difference of 10^6 causes the end of life phase to contribute the most to the terrestrial ecotoxicity.

3.2.2 IREC Battery

The LCIA results for the cradle to grave analysis of the IREC battery (from battery production through the use of the battery in an EV all the way to EOL) are shown in Table 3.6 where they are categorised by phase of life. The results are similar to the HELIS battery where the use phase dominates the GWP, ADP, AP, POCP, and primary energy demand categories while the battery production dominates the EP, HTP, FAETP, MAETP, TETP, and ODP categories. Since they are so similar, the impact categories won't be analysed in detail here and instead, the comparison between the two batteries will be gone through in the next section.

Table 3.6: LCIA results for the IREC battery (cradle to grave analysis) categorised by phase of life.

Impact Category	Total	Battery Production	Use	End of Life
GWP [kg CO ₂ -eq.]	1,46E+04	3,81E+03	1,08E+04	1,13E+01
ADP [MJ]	1,59E+05	4,41E+04	1,15E+05	5,53E+01
AP [kg SO ₂ -eq.]	4,32E+01	1,23E+01	3,08E+01	1,87E-02
EP [kg PO ₄ -eq.]	7,73E+00	4,54E+00	2,79E+00	4,02E-03
HTP [kg DCB-eq.]	2,37E+03	1,88E+03	4,92E+02	1,68E+00
FAETP [kg DCB-eq.]	7,92E+02	7,71E+02	2,16E+01	6,72E-02
MAETP [kg DCB-eq.]	4,01E+06	2,78E+06	1,23E+06	5,55E+02
TETP [kg DCB-eq.]	2,06E+01	8,34E+00	7,62E+00	4,68E+00
ODP [kg CFC 11-eq.]	5,09E-05	5,03E-05	4,79E-07	1,52E-11
POCP [kg C ₂ H ₄ -eq.]	2,81E+00	8,50E-01	1,97E+00	-1,63E-03
PED [MJ]	3,63E+05	1,09E+05	2,53E+05	6,55E+01

3.2.3 Battery Comparison

Table 3.7 below displays the total impacts for the two batteries to show the differences between them. The higher impacts are put in bold to clearly show in which categories which battery has more of an effect. As can be seen, the IREC battery has higher impacts in GWP, ADP, POCP, and primary energy. The HELIS battery has higher impacts in AP (although it's almost the same between the batteries), EP, HTP, FAETP, MAETP, TETP, and ODP. The differences between the batteries in the categories where the IREC battery has a higher impact are much smaller than the differences between the batteries in the categories where the HELIS battery has a higher impact. In other words, when the HELIS battery has a higher impact, it is a more significant difference. Since many of the parts are the same (anode, electrolyte, casing), these differences arise from the difference in cathodes and from different weights of the materials they do have in common.

A graph displaying the differences between the two batteries more visually is shown in Figures 3.10, 3.11, 3.12 and below.

As can be seen from Figure 3.10, the HELIS battery has a 12% lower global warming impact, however it has a higher human toxicity impact (almost 3X higher) as seen in Figure 3.11. From Figure 3.12, it can be seen that the IREC battery has a higher primary energy demand, but only by approximately

Table 3.7: LCIA results for the HELIS and IREC battery systems (cradle to grave analysis).

Impact Category	HELIS Battery	IREC Battery
GWP [kg CO ₂ -eq.]	1,28E+04	1,46E+04
ADP [MJ]	1,38E+05	1,59E+05
AP [kg SO ₂ -eq.]	4,33E+01	4,32E+01
EP [kg PO ₄ -eq.]	1,56E+01	7,33E+00
HTP [kg DCB-eq.]	6,96E+03	2,37E+03
FAETP [kg DCB-eq.]	2,87E+03	7,92E+02
MAETP [kg DCB-eq.]	1,05E+07	4,01E+06
TETP [kg DCB-eq.]	5,11E+01	2,06E+01
ODP [kg CFC 11-eq.]	1,40E-04	5,09E-05
POCP [kg C ₂ H ₄ -eq.]	2,75E+00	2,81E+00
PED [MJ]	2,83E+05	3,63E+05

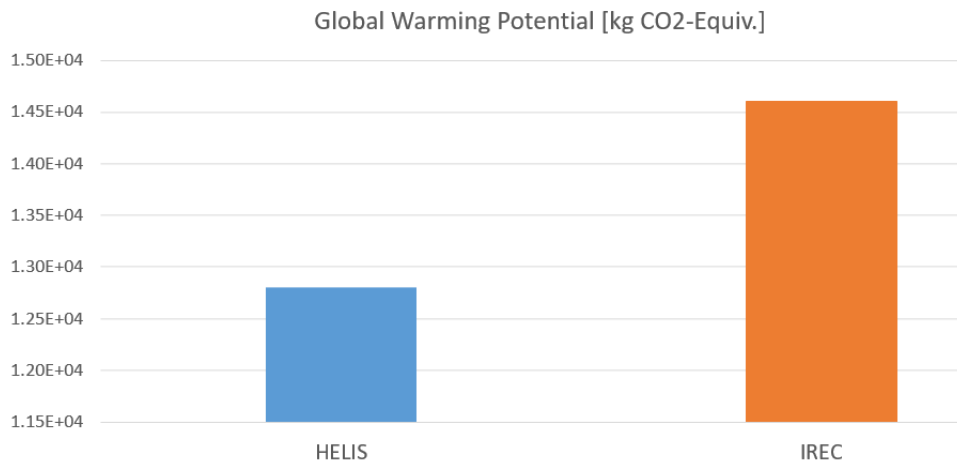


Figure 3.10: Graph showing the comparison between the HELIS and IREC batteries for global warming potential.

30%, not a very big difference considering the energy consumption of the cathode production is much higher than for the HELIS battery.

The differences in global warming, abiotic depletion, photochemical ozone creation, and primary energy are caused by the higher energy consumption the cathode production uses in the IREC battery. For example, in GWP, the IREC cathode contributes 22% to the overall impact whereas in the HELIS battery, the cathode only contributes 1%. Since the impacts of the individual materials in the cathodes are mostly equivalent (although the polyacrylonitrile and N,N-dimethylformamide in the IREC cathode have a bit higher impacts than the SBR and CMC in the HELIS cathode), these large differences are due to the vast difference in energy consumption of the cathodes.

The differences in acidification, eutrophication, human toxicity, freshwater ecotoxicity, marine ecotoxicity, terrestrial ecotoxicity, and ozone depletion are caused by the difference in battery pack material weights. In all of these impact categories, the battery pack was one of the major contributors, along with the electricity consumption during the use phase (which is the same between the two batteries because they are both 22 kWh batteries). Within the battery pack, the PCB has the highest effects, with steel and

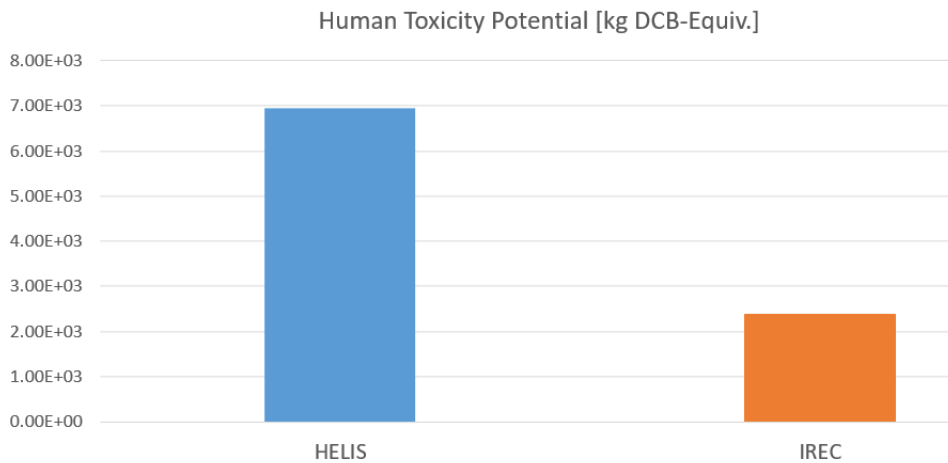


Figure 3.11: Graph showing the comparison between the HELIS and IREC batteries for human toxicity potential.

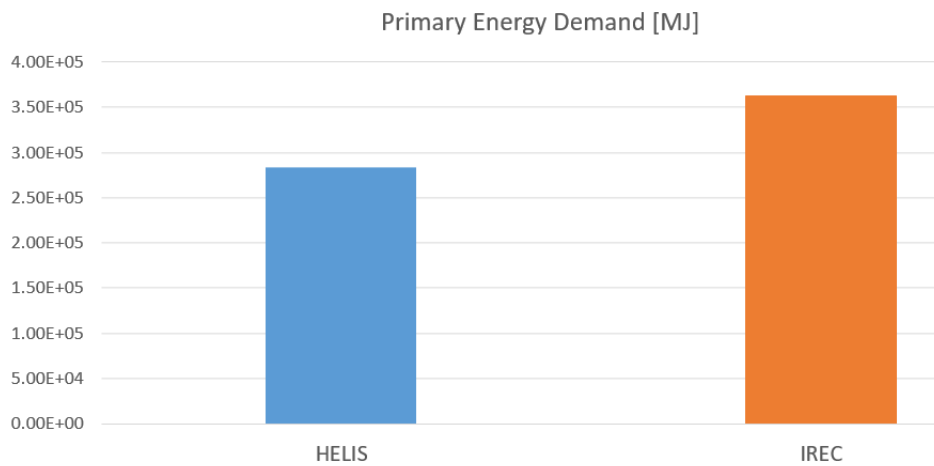


Figure 3.12: Graph showing the comparison between the HELIS and IREC batteries for primary energy demand.

then aluminium coming afterward. Since the battery pack of the HELIS battery is four times greater than the mass of the IREC battery pack (see Section 2.4.1), these categories have higher impacts from the HELIS battery. These are all due in the end to the lower energy density the HELIS cells perform at in comparison to the IREC cells.

3.3 Sensitivity Analyses

Due to the many assumptions inherent to this study because of the lack of necessary data, performing sensitivity analyses was critical. Three sensitivity analyses were performed: one on the energy density of the IREC battery, one on the energy consumption in the cathode production of the IREC battery, and one on the cathode binders used in the HELIS battery.

3.3.1 Energy Density

A sensitivity analysis was performed on the energy density of the IREC cylindrical battery since this energy density was not known and was subject to many assumptions and uncertainties. Thus, here the results are displayed for three energy densities tested: 787,5 Wh/kg (a 25% decrease in energy density), 525 Wh/kg (a 50% decrease from original), and 266 Wh/kg (the energy density of the HELIS cells and consequently almost exactly a 75% decrease in energy density from the original density). The results of these three new tests are displayed with the results of the original energy density tested (1050 Wh/kg) and with the HELIS battery results in Table 3.8 below and graphically for GWP in Figure 3.13. In Table 3.8, the impacts which remain lower than the HELIS battery impacts are bolded to highlight how low the energy density can go without having higher impacts than the HELIS battery.

Table 3.8: Results for the sensitivity analysis on energy density of the IREC cylindrical battery.

Impact Category	HELIS (266 Wh/kg)	IREC 1050 Wh/kg	IREC 787,5 Wh/kg	IREC 525 Wh/kg	IREC 266 Wh/kg
GWP [kg CO ₂ -eq.]	1,28E+04	1,46E+04	1,59E+04	1,84E+04	2,59E+04
ADP [MJ]	1,38E+05	1,59E+05	1,74E+05	2,03E+05	2,89E+05
AP [kg SO ₂ -eq.]	4,33E+01	4,32E+01	4,73E+01	5,55E+01	7,96E+01
EP [kg PO ₄ -eq.]	1,56E+01	7,33E+00	8,85E+00	1,19E+01	2,07E+01
HTP [kg DCB-eq.]	6,96E+03	2,37E+03	2,99E+03	4,25E+03	7,90E+03
FAETP [kg DCB-eq.]	2,87E+03	7,92E+02	1,05E+03	1,56E+03	3,06E+03
MAETP [kg DCB-eq.]	1,05E+07	4,01E+06	4,94E+06	6,79E+06	1,22E+07
TETP [kg DCB-eq.]	5,11E+01	2,06E+01	2,50E+01	3,37E+01	5,90E+01
ODP [kg CFC 11-eq.]	1,40E-04	5,09E-05	6,77E-05	1,01E-04	1,99E-04
POCP [kg C ₂ H ₄ -eq.]	2,75E+00	2,81E+00	3,10E+00	3,66E+00	5,31E+00
PED [MJ]	2,83E+05	3,63E+05	3,99E+05	4,72E+05	6,84E+05

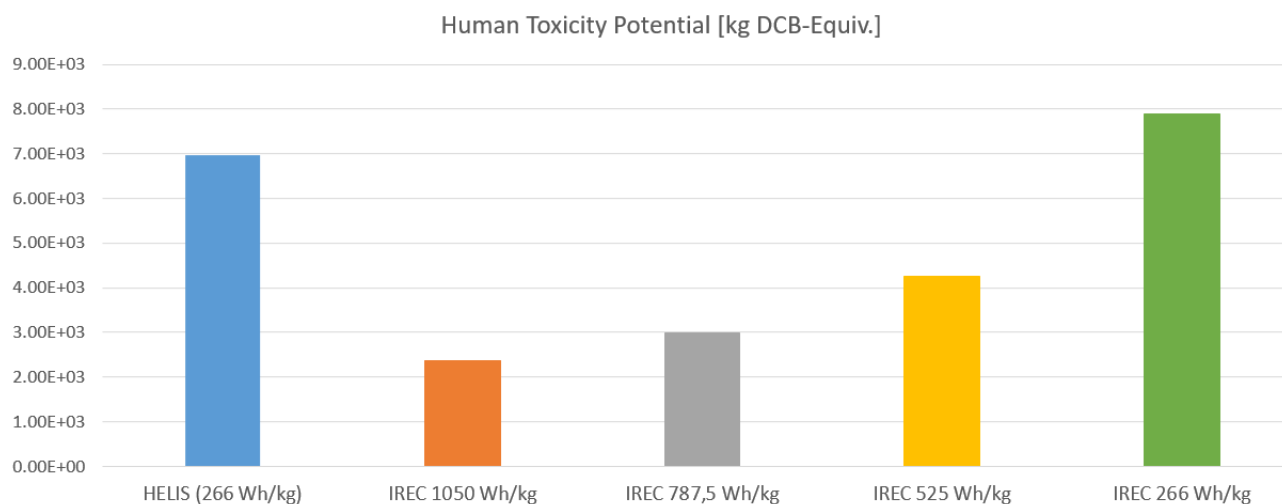


Figure 3.13: Graph showing the comparison between the four IREC batteries with varying energy densities and the HELIS battery for global warming potential.

As can be seen, there is a more or less proportionate increase in the impacts as the energy density decreases (due to the increase in material needed for the battery pack to reach 22 kWh). Some of the impact categories stay lower for the IREC battery as long as the energy density does not go down to 266 Wh/kg. Eutrophication, human toxicity, freshwater aquatic toxicity, marine aquatic toxicity, terrestrial

toxicity, and ozone depletion all are lower for the IREC battery at 525 Wh/kg than for the HELIS battery. From extrapolation, it was found that the energy density could decrease to 416 Wh/kg for the IREC battery to continue having a lower effect on EP than the HELIS battery and to 333 Wh/kg for the IREC battery to continue having a lower effect on HTP than the HELIS battery. But if the energy density of the IREC battery decreases until 266 Wh/kg (the same as the HELIS battery), all impacts are higher and there is no incentive to use this battery instead (due to the energy consumption in the cathode production).

3.3.2 Cathode Production Energy Consumption

Since the energy consumption in the production of the cathode of the IREC battery cells is the main factor causing such a large difference between the HELIS and IREC battery impacts, a sensitivity analysis was performed, decreasing the energy consumption of the IREC cathode to be equivalent to the energy consumption of the HELIS cathode (7,01E-02 MJ). Currently, the IREC cathodes made in-house from scratch are produced one at a time, causing the energy consumption per battery cell to be incredibly high. This sensitivity analysis proposes an industrial-scale production process so that many more cathodes can be produced at once and thus the energy consumption per cell decreases drastically. The results, given in the total battery LCA (cradle to grave) are represented below in Table 3.9 and are also shown graphically for the freshwater aquatic ecotoxicity in Figure 3.14.

Table 3.9: Results for the sensitivity analysis on cathode production energy consumption.

Impact Category	HELIS Battery	IREC Battery Low Energy
GWP [kg CO ₂ -eq.]	1,28E+04	1,14E+04
ADP [MJ]	1,38E+05	1,22E+05
AP [kg SO ₂ -eq.]	4,33E+01	3,45E+01
EP [kg PO ₄ -eq.]	1,56E+01	6,38E+00
HTP [kg DCB-eq.]	6,96E+03	2,20E+03
FAETP [kg DCB-eq.]	2,87E+03	7,85E+02
MAETP [kg DCB-eq.]	1,05E+07	3,72E+06
TETP [kg DCB-eq.]	5,11E+01	1,89E+01
ODP [kg CFC 11-eq.]	1,40E-04	4,95E-05
POCP [kg C ₂ H ₄ -eq.]	2,75E+00	2,20E+00
PED [MJ]	2,83E+05	2,62E+05

As can be seen, once the energy consumption is equated for the two batteries, the IREC battery then has lower impacts in all categories, due to the fact that the energy density is higher and thus less material is needed. The largest difference occurs in the freshwater aquatic ecotoxicity category, with the IREC battery having a 73% lower impact than the HELIS battery. It is yet to be seen if the energy consumption for the cathode production of the IREC cells could actually be reduced enough to see these kinds of results but if it is possible and the energy density remains higher than the HELIS cells, it makes sense to use the IREC cell chemistry.

Additionally, the HELIS battery uses much more aluminium in its cathode and since aluminium is a

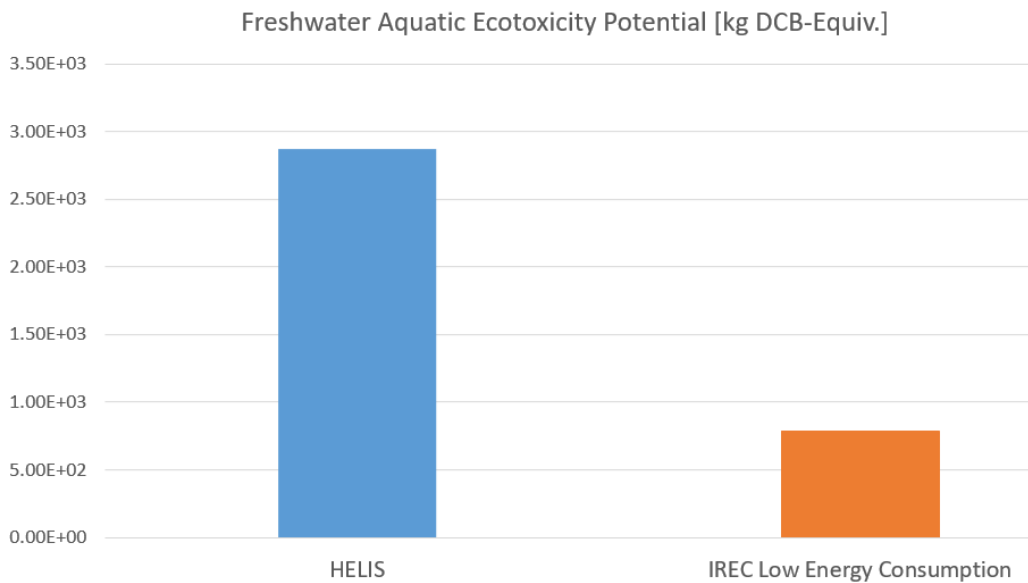


Figure 3.14: Graph showing the comparison between the two batteries when the energy consumption of the cathode of the IREC battery is equated to that of the HELIS battery for freshwater aquatic ecotoxicity.

very high-impact metal, this contributes to the difference in the two batteries concerning the cathode once the energy consumption is equated. The HELIS battery cell has 36 g of aluminium while the IREC battery cell has less than 8 g of aluminium - this difference of over 4X contributes to a significant difference in cell production impacts.

3.3.3 Cathode Binders

Although cathode binders are not used in the IREC battery cells, the HELIS cells do use them and they are a point of investigation in the project. Thus, a sensitivity analysis was performed on two cathode binders that have been used in the cell prototypes: SBR and CMC in water and PVDF in NMP. The comparison of these two binders has been performed in other studies as well and the results here were compared with those in literature - in this way, it also assured that the results coming from GaBi Professional are in line with results found in other studies. The results are shown below in Table 3.10 and graphically for GWP in Figure 3.15.

As can be seen, cathode binder 2 of PVDF in NMP has higher impacts in all categories. The all-water-based binder provides a 17% reduction in global warming potential and a 95% reduction in ozone depletion potential from the organic binder - Peters, et. al. got similar results of a 8.6% reduction in GWP and almost one order of magnitude change in ODP [22]. However, while Peters, et. al. saw relatively little changes in the other impact categories, here there is a 57% decrease in eutrophication potential as well as 89% in freshwater aquatic toxicity [22]. Thus it is proven that SBR and CMC in water is a more environmental choice of cathode binder.

The HELIS project continues to investigate new types of cathode binders; thus once a new binder is tested, it can be analysed along with SBR and CMC in water to see which is more environmentally benign.

Table 3.10: Results for the sensitivity analysis on cathode binder in the HELIS cells.

Impact Category	Cathode Binder 1 (SBR+CMC in water)	Cathode Binder 2 (PVDF in NMP)
GWP [kg CO ₂ -eq.]	5,46E-01	6,57E-01
ADP [MJ]	8,91E+00	9,59E+00
AP [kg SO ₂ -eq.]	2,17E-03	2,89E-03
EP [kg PO ₄ -eq.]	1,63E-04	3,81E-04
HTP [kg DCB-eq.]	1,50E+00	1,57E+00
FAETP [kg DCB-eq.]	4,92E-03	4,75E-02
MAETP [kg DCB-eq.]	7,38E+02	9,24E+02
TETP [kg DCB-eq.]	1,04E-03	1,43E-03
ODP [kg CFC 11-eq.]	5,12E-10	9,92E-09
POCP [kg C ₂ H ₄ -eq.]	1,56E-04	1,97E-04
PED [MJ]	1,17E+01	1,27E+01

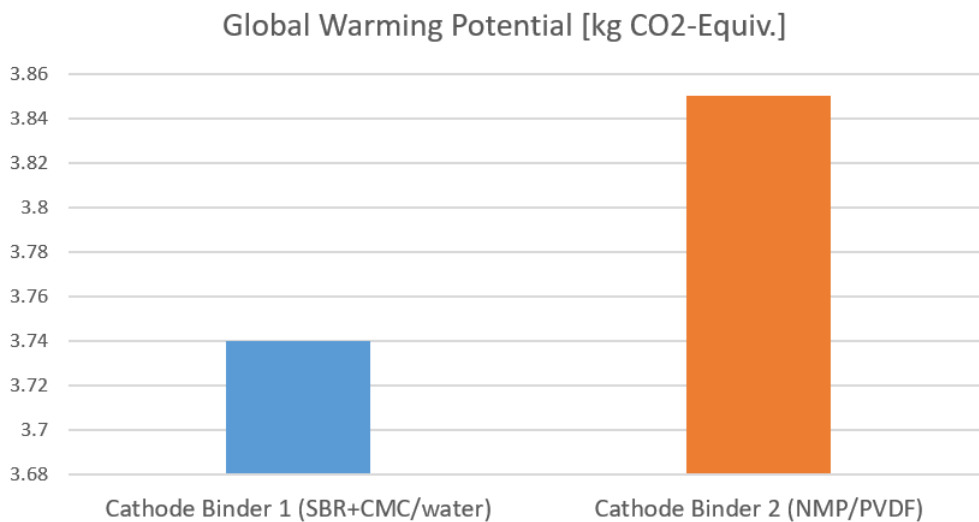


Figure 3.15: Graph showing the comparison between the two cathode binders in the HELIS battery cell for global warming potential.

Chapter 4

Conclusions

Here the achievements of the study are described with a summary of the results obtained and lessons learned along the process. Future work is presented afterwards.

4.1 Achievements

A LCA study has been successfully performed on two different Li-S cells and battery systems. Various materials have been pinpointed in the battery cells that have higher impacts and which battery ultimately would be more sustainable in the application of electromobility has been investigated.

Regarding the first objective, a cradle to gate analysis of the cell production, it was seen that the materials with the highest environmental impacts were shown to be lithium, stainless steel, and aluminium. If these materials can be decreased in mass or even replaced with more environmental materials, the batteries would have fewer impacts.

Regarding the second objective, a cradle to grave analysis to compare the two battery systems through their production, use in an EV, and EOL, it has been shown that for now, the HELIS battery has a lower carbon footprint although the IREC battery is more sustainable regarding other impact categories such as human toxicity, ecotoxicity, and ozone depletion. However, if the IREC battery can achieve lower energy consumption for the production of the cathode, it would become the superior battery chemistry for all impact categories as long as the energy density stays higher than the HELIS battery energy density.

The battery pack materials were among the most environmentally intensive materials in the cradle to grave study, especially when it came to marine ecotoxicity. Since the battery pack was assumed from literature, a more adequate pack with BMS should be investigated and used in future LCAs to provide more updated results.

Additionally, it was shown through a sensitivity analysis that an all-water-based cathode binder (SBR and CMC) is proven to be more environmentally sustainable than an organic cathode binder (PVDF in NMP) that is most often used in batteries.

Since these batteries are still very much in the research phase, a completely adequate LCA is impossible at this stage. However, this LCA study provides a good basis for when the batteries have matured

and performance is proven.

4.1.1 Summary of Results

In the HELIS battery cell, the primary materials dominated all impact categories, from 90% up to 99,9%, whereas production and transport had very small, if not negligible, contributions. The anode most clearly had most of the impact of the HELIS cell, from 51% contribution up to 92%, although the cathode and electrolyte did contribute to human toxicity due to the aluminium and ethylene glycol dimethyl ether.

In the IREC battery cell, the production dominated almost all impact categories, from 57% up to 99,5%, although ozone layer depletion was dominated by primary materials due to the stainless steel parts involved in the cell production. Whereas the HELIS battery cell impacts were dominated by the primary materials, the IREC battery cell impacts are dominated by production due to the highly energy-intensive cathode production process. In both cells, the transport stream has negligible effects despite the high amounts of transport needed (in the HELIS cell production, the transport of the various parts between the partners and in the IREC cell production, the transport of the coin cell parts from Japan).

Among the two battery systems the effects were pretty evenly split between the battery production phase and the use phase, with the production phase having the highest effects on EP, HTP, FAETP, MAETP, TETP, and ODP and the use phase having the highest effects on GWP, ADP, AP, POCP, and PED. When the two batteries were compared, the HELIS battery had a lower GWP as well as lower ADP, POCP, and PED (due to the higher energy consumption in the cathode production process for the IREC battery), but the IREC battery had lower effects on AP, EP, HTP, FAETP, MAETP, TETP, and ODP (due to the difference in battery pack material weights). Since the differences in GWP, ADP, POCP, and PED are caused by the higher energy consumption in the cathode production process for the IREC battery, a sensitivity analysis was performed on decreasing this energy consumption.

The category with the highest impacts was found to be MAETP due to the battery pack materials, like PCB and stainless steel which have much higher effects on marine ecotoxicity than on freshwater ecotoxicity or any other impact category.

From the sensitivity analyses performed, it was found that the energy density of the IREC battery could decrease to 525 Wh/kg or even a bit lower and still maintain lower impacts in many categories such as EP, HTP, and ODP than the HELIS battery but that if the IREC battery's energy density decreased to 266 Wh/kg (that of the HELIS battery), its impacts would be higher in every category (due to the energy consumption in the cathode). Additionally, if the energy consumption of the cathode production process for the IREC battery were decreased to be equivalent to that of the HELIS battery, then the IREC battery would have lower impacts in all categories, from a mere 7% decrease in primary energy up to a 73% decrease in FAETP. Finally, it was proven that SBR and CMC in water is a more sustainable binder to use than PVDF in NMP, providing reductions of up to 95% in ODP.

4.1.2 Lessons Learned

This study involved the extensive use of GaBi Professional Software, as well as extensive literature research on various batteries in the field of energy storage.

As well as providing a good handle on the most popular LCA tools, the research on two batteries that are very much still in the investigative stage helped to understand the process of battery maturity and the eventual release to market. Li-S batteries still have a long way to come to become the new replacement for Li-ion batteries in EVs, but this study has provided another look into the research process and where some aspects may be improved upon.

4.2 Future Work

There is much future work that can be done here. For one, more sensitivity analyses could be performed, some of which could include varying the battery power capacity (22 kWh, 50 kWh, 60 kWh, etc.), varying the country of production and use (China and Sweden for example, in addition to the European average), and changing battery pack materials. Also, the sensitivity analyses performed on the IREC batteries here (energy density and cathode production energy consumption) could be combined to see the results when the energy consumption is optimised but the energy density decreases.

Additionally, a LCC analysis could be performed to see which battery is more economically sustainable. While there was not adequate financial data to perform it here, it would be an interesting study to pair with the LCA to see if the battery that is environmentally superior is also financially superior.

Research on a BMS for the HELIS battery is ongoing, so once one is designed, a LCA could be performed with this new data to see how the results change. In general, as these batteries undergo further investigation and perform better, LCA studies with the updated materials and processes could show more reliable and interesting results.

Bibliography

- [1] R. Dominko. HELIS Project Proposal, October 2014.
- [2] Y. Deng, J. Li, T. Li, X. Gao, and C. Yuan. Life cycle assessment of lithium sulfur battery for electric vehicles. *Journal of Power Sources*, 343:284–295, March 2017. doi:10.1016/j.jpowsour.2017.01.036.
- [3] S. Brauer. They Not Only Live Once - Towards Product-Service Systems for Repurposed Electric Vehicle Batteries. In V. Nissen, D. Stelzer, S. Straburger, and D. Fischer, editors, *Service Systems Engineering*, pages 1300–1310, Technische Universitat Ilmenau 09, March 2016. Multikonferenz Wirtschaftsinformatik (MKWI). ISBN 978-3-86360-132-4.
- [4] L. Casals and B. García. Assessing Electric Vehicles Battery Second Life Remanufacture and Management. *Journal of Green Engineering*, 6:77–98, August 2016. doi:10.13052/jge1904-4720.614.
- [5] SETAC. Society of Environmental Toxicology and Chemistry, 2017. URL <https://www.setac.org/>. Online; accessed 09-March-2017.
- [6] ISO. International Organization for Standardization: Standards catalogue, 2017. URL <https://www.iso.org/committee/54854/x/catalogue/>. Online; accessed 09-March-2017.
- [7] P. International. GaBi Paper Clip Tutorial, 2011. URL http://www.gabi-software.com/uploads/media/Paper_Clip_Tutorial_Handbook_Part1.pdf. Online; accessed 09-March-2017.
- [8] J. Guinée, M. Gorrée, R. H. G. Huppes, R. Kleijn, A. de Koning, L. van Oers, A. W. Sleeswijk, S. Suh, H. U. de Haes, H. de Bruijn, R. van Duin, and M. Huijbregts. *Handbook on life cycle assessment. Operational guide to the ISO standards.*, volume 7. Kluwer Academic Publishers, Dordrecht, first edition, 2002. ISBN 1-4020-0228-9; doi:10.1007/0-306-48055-7.
- [9] thinkstep. GaBi Professional [Software], 2017. URL <http://www.gabi-software.com/international/software/>. Online; accessed 09-March-2017.
- [10] E. Commission. Joint Research Centre: European Life Cycle Database, 2017. URL <http://eplca.jrc.ec.europa.eu/ELCD3/>. Online; accessed 09-March-2017.
- [11] NREL. U.S. Life Cycle Inventory Database, 2013. URL <http://www.nrel.gov/lci/>. Online; accessed 09-March-2017.

- [12] EPD. The International EPD System, 2017. URL <http://www.environdec.com/>. Online; accessed 09-March-2017.
- [13] X. Ji and L. Nazar. Advances in Li-S Batteries. *Journal of Materials Chemistry*, 20:9821–9826, September 2010. doi:10.1039/b925751a.
- [14] A. Manthiram, Y. Fu, and Y.-S. Su. Challenges and Prospects of Lithium-Sulfur Batteries. *Accounts of Chemical Research*, 46(5):1125–1134, May 2013. doi:10.1021/ar300179v.
- [15] J. Cobb. OXIS Jump-Starts First Commercialization Of Lithium-Sulfur Batteries, 2013. URL <http://www.hybridcars.com/oxis-jump-starts-first-commercialization-of-lithium-sulfur-batteries/>. Online; accessed 24-May-2017.
- [16] Y. Diao, K. Xie, S. Xiong, and X. Hong. Analysis of Polysulfide Dissolved in Electrolyte in Discharge-Charge Process of Li-S Battery. *Journal of the Electrochemical Society*, 159(5):A421–A425, January 2012. doi:10.1149/2.060204jes.
- [17] D. Deng. Li-ion batteries: basics, progress, and challenges. *Energy Science & Engineering*, 3: 385–418, September 2015. doi:10.1002/ese3.95.
- [18] N. Nitta, F. Wu, J. Lee, and G. Yushin. Li-ion battery materials: present and future. *Materials Today*, 18:252–264, June 2015. doi:10.1016/j.mattod.2014.10.040.
- [19] K. Patel. Lithium-Sulfur Battery: Chemistry, Challenges, Cost, and Future. *Journal of Undergraduate Research*, 9:39–42, August 2016. doi:10.5210/jur.v9i2.7553.
- [20] S. Ahmed, P. Nelson, K. Gallagher, N. Susarla, and D. Dees. Cost and energy demand of producing nickel manganese cobalt cathode material for lithium ion batteries. *Journal of Power Sources*, 342: 733–740, January 2017. doi:10.1016/j.jpowsour.2016.12.069.
- [21] M. Goedkoop, R. Heijungs, M. Huijbregts, A. Schryver, J. Struijs, and R. van Zelm. ReCiPe 2008 Report I: Characterisation. Technical report, Ruimte en Milieu, July 2012.
- [22] J. Peters, D. Buchholz, S. Passerini, and M. Weil. Life Cycle Assessment of Sodium-ion Batteries. *Energy & Environmental Science*, 9:1744–1751, March 2016. doi:10.1039/c6ee00640j.
- [23] U. Leiden. CML-IA Characterisation Factors, 2016. URL <https://www.universiteitleiden.nl/en/research/research-output/science/cml-ia-characterisation-factors#downloads>. Online; accessed 05-July-2017.
- [24] T. Ekvall and A.-M. Tillman. Open-loop recycling: Criteria for allocation procedures. *The International Journal of Life Cycle Assessment*, 2:155–162, September 1997. doi:10.1007/BF02978810.
- [25] M. Romare and M. Henriksson. Comparative LCA study and life cycle analysis. Collaborative project, Volvo Technology AB, September 2016.

- [26] H. Corp. Products: Coin Cell Kit. URL http://www.hohsen.co.jp/en/products/category.php?mg_id=15. Online; accessed 24-May-2017.
- [27] C. Donoso and J. Biendicho, 2017. Personal correspondence.
- [28] B. University. BU-1003: Electric Vehicle (EV), 2016. URL http://batteryuniversity.com/learn/article/electric_vehicle_ev. Online; accessed 24-May-2017.
- [29] P. Nelson, K. Gallagher, I. Bloom, and D. Dees. *Modeling the Performance and Cost of Lithium-Ion Batteries for Electric Drive Vehicles*. Argonne National Laboratory, second edition, December 2012.
- [30] Y. Deng, J. Li, T. Li, X. Gao, and C. Yuan. *Life Cycle Assessment of Lithium Sulfur Battery for Electric Vehicles Supporting Information*, October 2012.
- [31] T. Hawkins, B. Singh, G. Majeau-Bettez, and A. Stromman. Comparative Environmental Life Cycle Assessment of Conventional and Electric Vehicles. *Journal of Industrial Ecology*, 17:53–64, February 2013. doi:10.1111/j.1530-9290.2012.00532.x.
- [32] Eurostat. Supply, Transformation and Consumption of Electricity - Annual Data, 2017. URL http://appsso.eurostat.ec.europa.eu/nui/show.do?dataset=nrg_105a&lang=en. Online; accessed 24-July-2017.

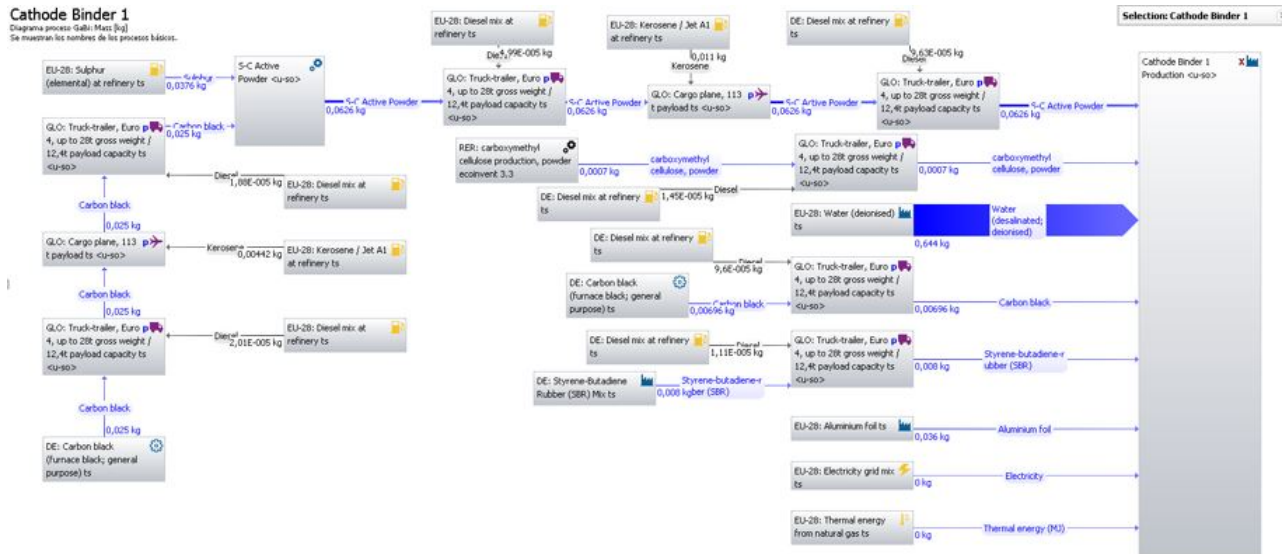


Figure A.2: The GaBi process flow is displayed for the cathode of the HELIS battery.

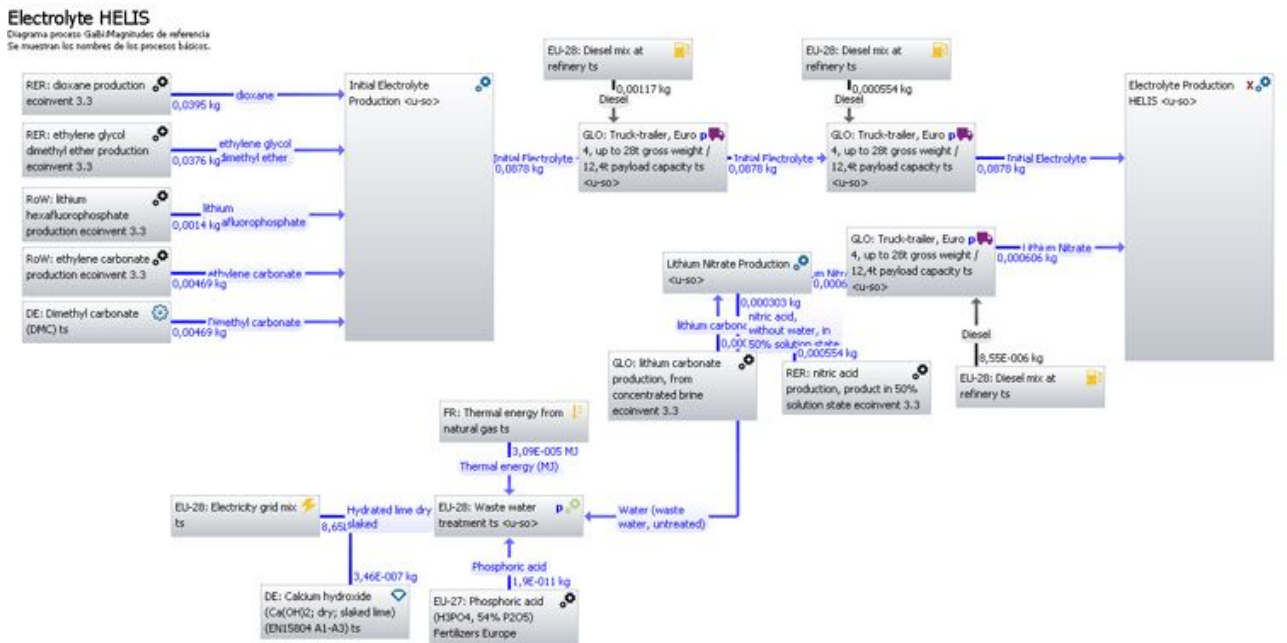


Figure A.3: The GaBi process flow is displayed for the electrolyte of the HELIS battery.

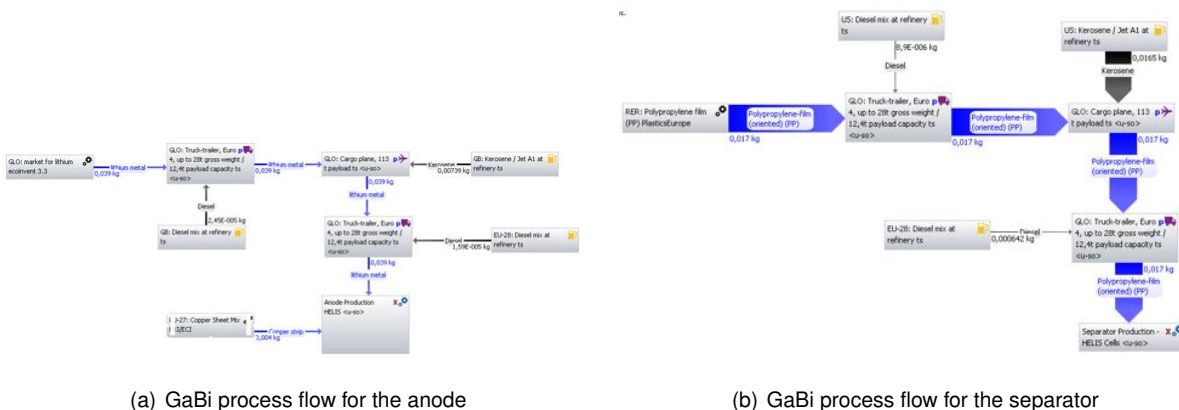


Figure A.4: The GaBi process flows are displayed for the anode of the HELIS battery [left] and the separator of the HELIS battery [right].

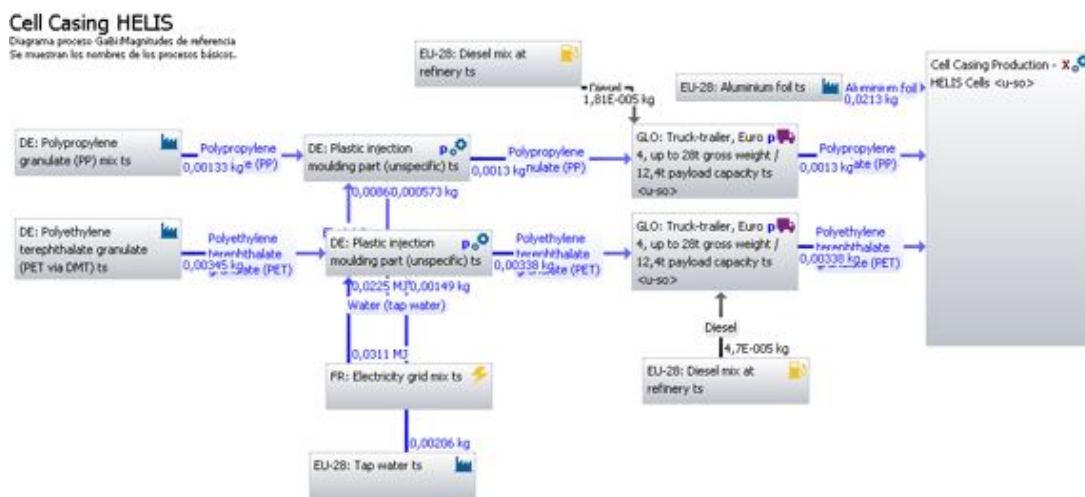


Figure A.5: The GaBi process flow is displayed for the cell casing of the HELIS battery.



Figure A.6: The GaBi process flow is displayed for the battery pack (the same materials were used for the two battery systems).

Appendix B

GaBi Process Flows: IREC Battery

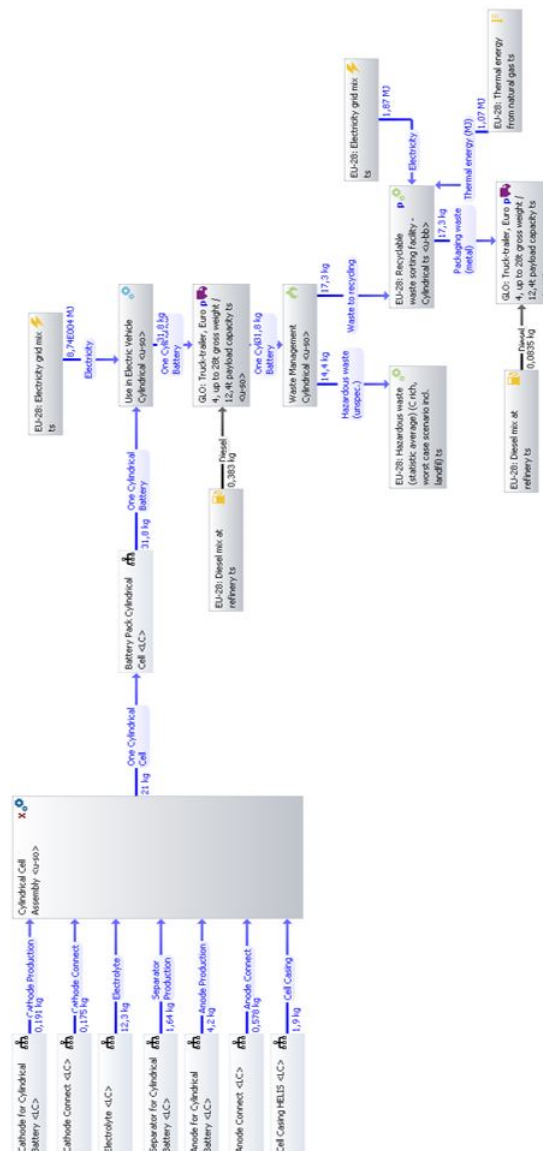


Figure B.1: The GaBi process flow is displayed for the cradle to grave model of the IREC battery.

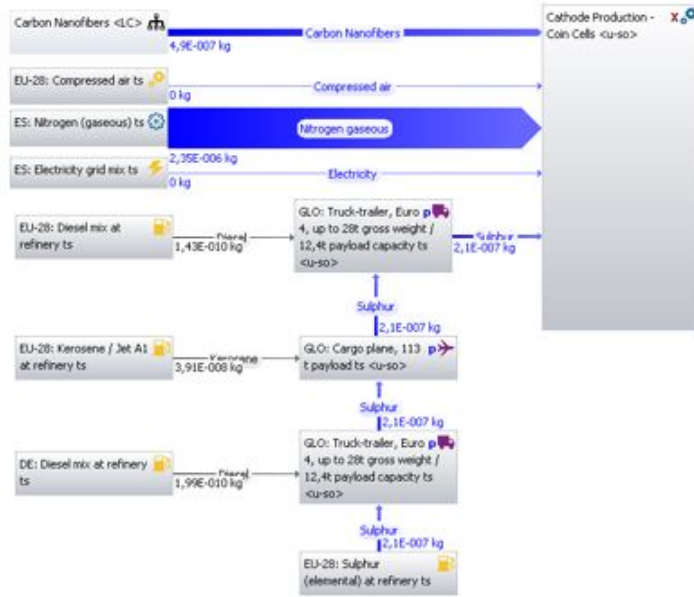


Figure B.2: The GaBi process flow is displayed for the cathode of the IREC battery.

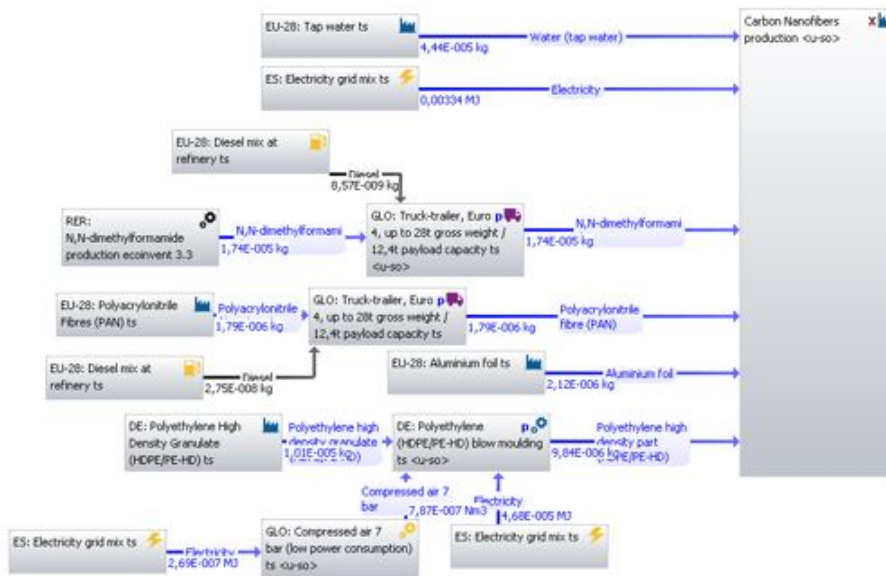


Figure B.3: The GaBi process flow is displayed for the carbon nanofibers produced for the cathode of the IREC battery.



(a) GaBi process flow for the anode

(b) GaBi process flow for the separator

Figure B.4: The GaBi process flows are displayed for the anode of the IREC battery [left] and the separator of the IREC battery [right].



Figure B.5: The GaBi process flow is displayed for the electrolyte of the IREC battery. It only consists of transport since it is the same electrolyte used as in the HELIS battery.

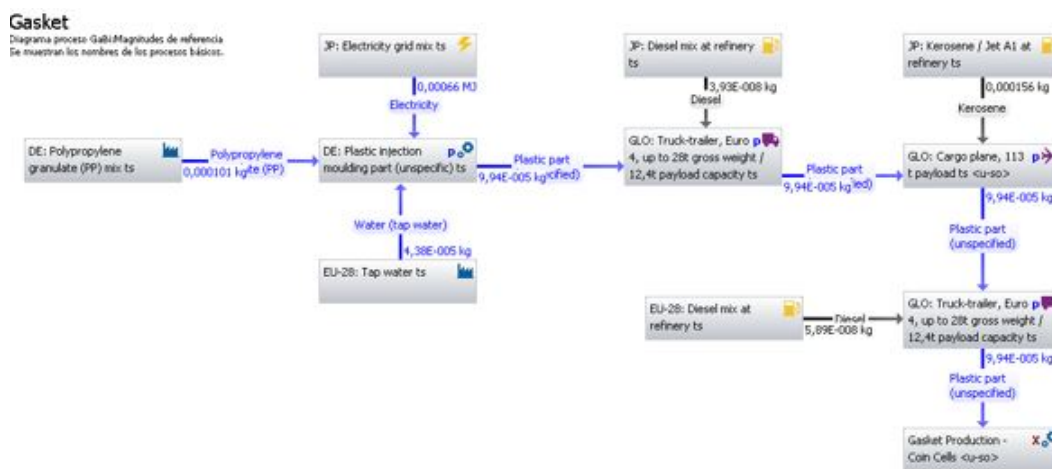


Figure B.6: The GaBi process flow is displayed for the gasket of the IREC battery.

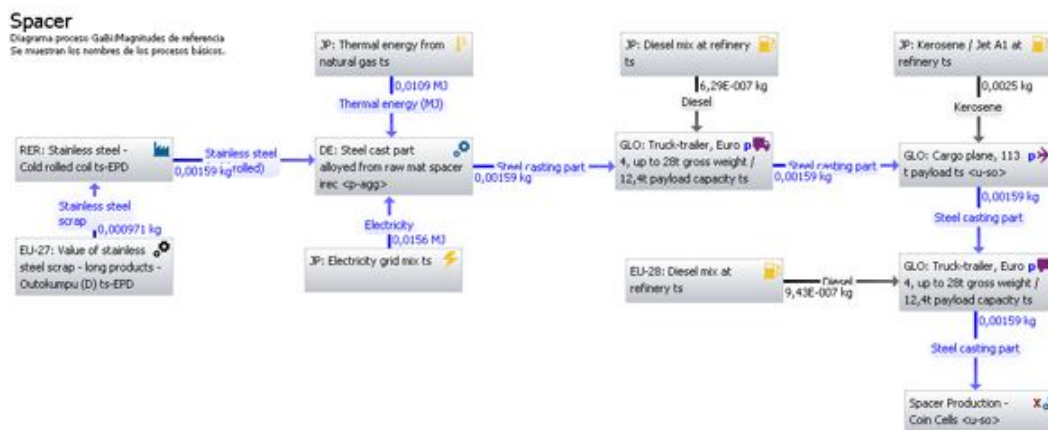


Figure B.7: The GaBi process flow is displayed for the spacer of the IREC battery.

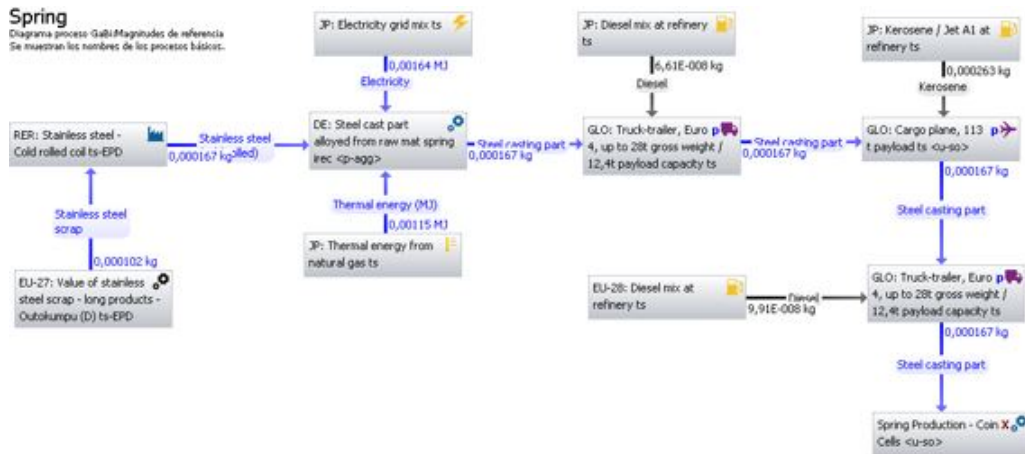


Figure B.8: The GaBi process flow is displayed for the spring of the IREC battery.

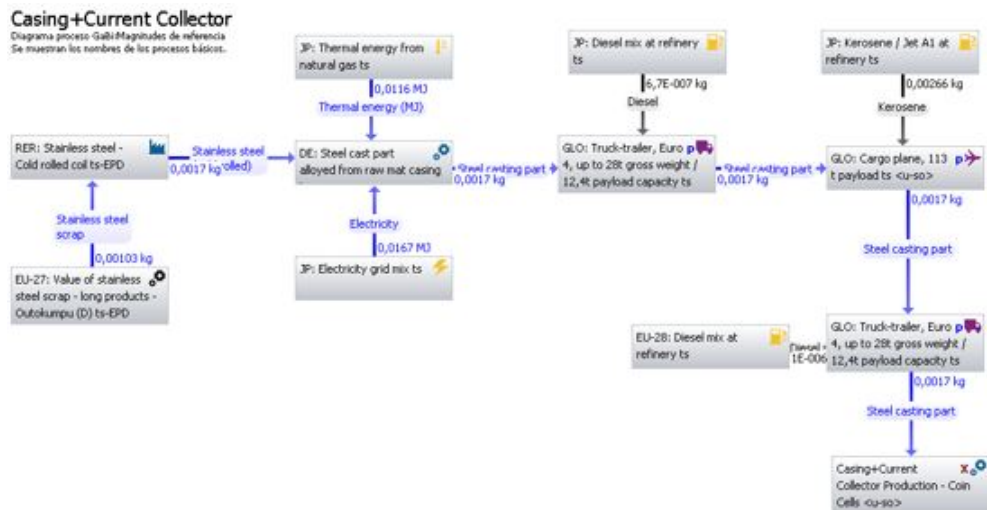


Figure B.9: The GaBi process flow is displayed for the cell casing of the IREC battery.

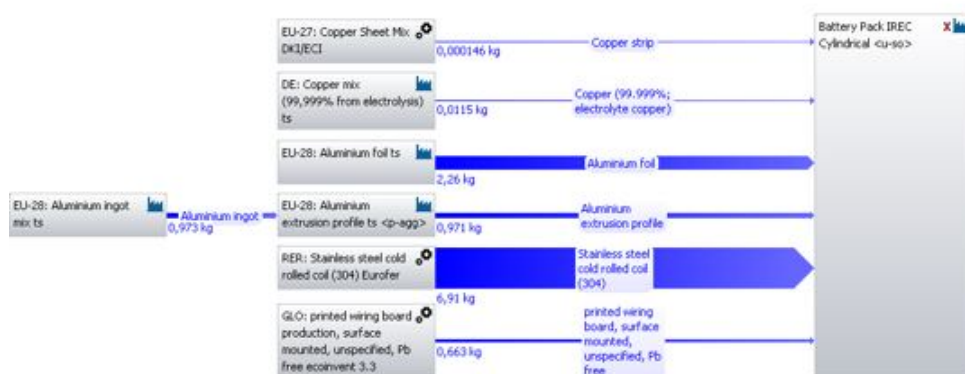


Figure B.10: The GaBi process flow is displayed for the battery pack of the IREC battery.